

Effects of the maternal and fetal proteome on birth weight: a Mendelian randomization analysis

Nancy McBride^{*1,2}, Alba Fernández-Sanlés^{1,3}, Marwa Al Arab², Tom A. Bond^{1,2,11}, Jie Zheng^{5,6}, Maria C. Magnus⁷, Elizabeth C. Corfield^{1,8,9}, Gemma L Clayton^{1,2}, Liang-Dar Hwang¹¹, Robin N. Beaumont¹⁰, David M. Evans^{1,4,11}, Rachel M. Freathy¹⁰, Tom R. Gaunt^{1,2}, Deborah A Lawlor^{1,2}, Maria Carolina Borges^{1,2}

¹MRC Integrative Epidemiology Unit at the University of Bristol

²Population Health Science, Bristol Medical School, University of Bristol

³MRC Unit for Lifelong Health and Ageing, University College London

⁴Frazer Institute, University of Queensland, Brisbane, QLD, Australia

⁵Department of Endocrine and Metabolic Diseases, Shanghai Institute of Endocrine and Metabolic Diseases, Ruijin Hospital, Shanghai Jiao Tong University School of Medicine, Shanghai, 200025, China

⁶Shanghai National Clinical Research Center for Metabolic Diseases, Key Laboratory for Endocrine and Metabolic Diseases of the National Health Commission of the PR China, Shanghai Key Laboratory for Endocrine Tumor, State Key Laboratory of Medical Genomics, Ruijin Hospital, Shanghai Jiao Tong University School of Medicine, Shanghai, 200025, China

⁷Centre for Fertility and Health, Norwegian Institute of Public Health, Oslo, Norway

⁸Psychiatric Genetic Epidemiology Group, Research Department, Lovisenberg Diaconal Hospital, Oslo, Norway

⁹PsychGen Centre for Genetic Epidemiology and Mental Health, Norwegian Institute of Public Health, Oslo, Norway

¹⁰Department of Clinical and Biomedical Sciences, Faculty of Health and Life Sciences, University of Exeter, Exeter, UK

¹¹Institute for Molecular Bioscience, The University of Queensland, Brisbane, QLD, Australia

*Corresponding author

nancy.mcbride@bristol.ac.uk

1 **Abstract**

2 Background

3 Fetal growth is an important indicator of survival, regulated by maternal and fetal genetic and
4 environmental factors. However, little is known about the underlying molecular mechanisms.
5 Proteins play a major role in a wide range of biological processes and could provide key
6 insights into maternal and fetal molecular mechanisms regulating fetal growth.

7 Method

8 We used intergenerational two-sample Mendelian randomization to explore the effects of
9 1,139 maternal and fetal genetically-instrumented plasma proteins on birth weight. We used
10 genome-wide association summary data from the Early Growth Genetics (EGG) consortium
11 (n=406,063 with maternal and/or fetal genotype), with independent replication in the
12 Norwegian Mother, Father and Child Cohort Study (MoBa; n=74,932 mothers and n=62,108
13 offspring). Maternal and fetal data were adjusted for the correlation between fetal and
14 maternal genotype, to distinguish their independent genetic effects.

15 Results

16 We found that higher genetically-predicted maternal levels of NEC1 increased birth weight
17 (mean-difference: 12g (95% CI [6g, 18g]) per 1 standard deviation protein level) as did
18 PRS57 (20g [10g, 31g]) and ULK3 (140g [81g, 199g]). Higher maternal levels of Galectin_4
19 decreased birth weight (-206g [-299g, -113g]). In contrast, in the offspring, higher
20 genetically-predicted offspring levels of NEC1 decreased birth weight (-10g [-16g, -5g]),
21 alongside sLeptin_R (-8g [-12g, -4g]), and UBS3B (-78g [-116g, -41g]). Higher fetal levels of
22 Galectin_4 increased birth weight (174g [89g, 258g]). We replicated these results in MoBa,
23 and found supportive evidence for shared causal variants from genetic colocalization
24 analyses and protein-protein network associations.

25 Conclusions

26 We find strong evidence for causal effects, sometimes in opposing directions, of maternal
27 and fetal genetically-instrumented proteins on birth weight. These provide new insights into
28 maternal and fetal molecular mechanisms regulating fetal growth, involving glucose
29 metabolism, energy balance, and vascular function that could be used to identify new
30 intervention targets to reduce the risk of fetal growth disorders, and their associated adverse
31 maternal and fetal outcomes.

32 Keywords: fetal growth, birth weight, proteomics, molecular mechanisms, Mendelian
33 randomization, pregnancy, MoBa

34

35 Introduction

36 Birth weight is a valuable and widely used measure of fetal growth. Healthy fetal growth is
37 essential to minimise adverse perinatal health outcomes, including miscarriage, stillbirth,
38 preterm birth and associated neonatal and infant morbidity and mortality (1-7). Large-scale
39 genome-wide association studies (GWAS) have revealed hundreds of genomic regions
40 independently associated with birth weight (2, 3, 8-10). In addition, these GWAS have
41 uncovered a complex interplay between maternal and fetal genomes (8, 9), in which some
42 genetic variants have maternal or fetal-specific effects on birth weight, whereas other genetic
43 variants have both maternal and fetal effects, sometimes in opposite directions. Despite
44 these advances in mapping fetal and maternal genetic variants, understanding the molecular
45 mechanisms underpinning fetal growth remains a challenge (6).

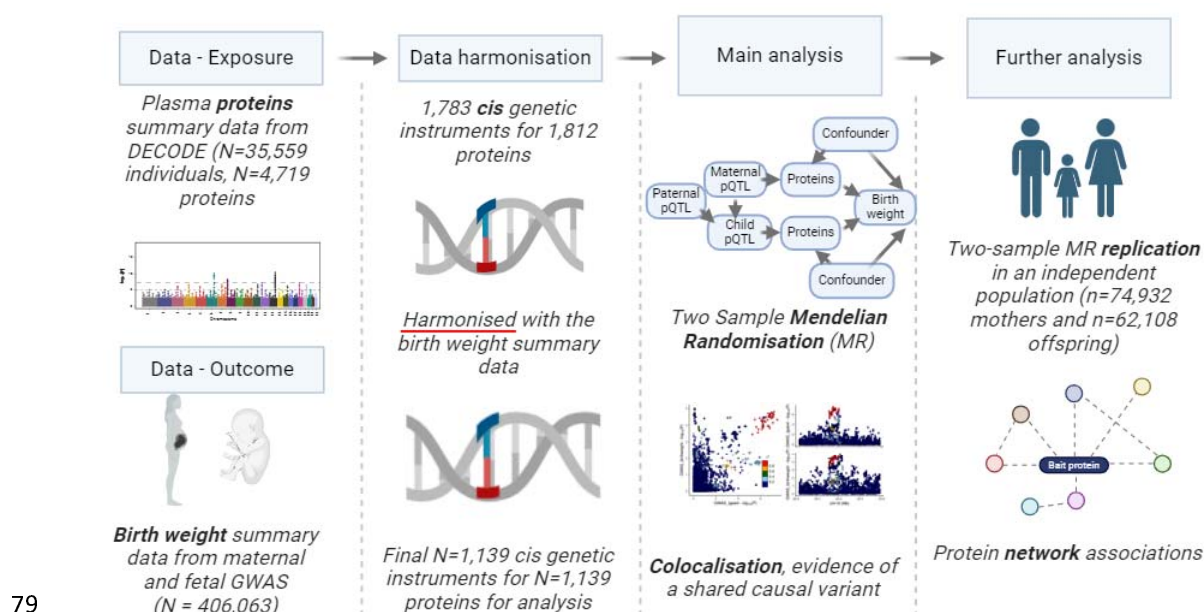
46 Proteins play a major role in a wide range of biological processes (11). They are essential for
47 cellular growth and repair, and could provide key insights into maternal and fetal molecular
48 mechanisms regulating fetal growth (10). Mendelian Randomization (MR) is a method which
49 uses genetic variants associated with exposures as instrumental variables, to test the effect
50 of those exposures on human traits and diseases. The method aims to mitigate causal
51 effects being biased due to confounding and reverse causation that may explain
52 conventional observational associations. Previous MR studies have established causality of
53 maternal modifiable factors on offspring birth weight, including higher maternal adiposity and
54 higher maternal circulating glucose levels on higher birth weight, and smoking and higher
55 blood pressure on lower birth weight (12) (13, 14) (5) (15). They have also provided novel
56 insights, such as a potential effect of higher maternal glutamine levels on higher birth weight
57 (5) and metabolically favourable adiposity on lower birth weight (16). As such, MR and
58 proteomics can be integrated to explore maternal and fetal proteins regulating fetal growth
59 by using genetic variants associated with protein levels (i.e., protein quantitative trait loci -
60 pQTL) as instrumental variables. As most drug targets are proteins, identifying the effects of
61 maternal circulating proteins on birth weight could identify targets for drug development that
62 might prevent fetal growth restriction and over-growth, and their associated adverse
63 pregnancy and perinatal outcomes.

64 The aim of this study was to identify causal effects of maternal and fetal proteins on birth
65 weight to highlight underlying molecular mechanisms. To achieve that, we used two-sample
66 MR, in which large-scale GWAS of plasma proteomics and birth weight were combined to
67 examine the causal effect of plasma proteins on offspring birth weight.

68

69 Methods

70 We performed a two-sample MR study to identify maternal and fetal effects of plasma
 71 proteins on offspring birthweight, examining both maternal and fetal genetic effects
 72 (n=406,063 with maternal and/or fetal genotype). For proteins passing multiple testing
 73 correction (FDR p-value < 5%), we tested whether results replicated in an independent
 74 sample (n=74,932 mothers and n=62,108 offspring) and investigated whether MR results
 75 could be confounded by linkage disequilibrium using genetic colocalization. For proteins
 76 which had discovery and replication evidence, and no evidence against colocalization, we
 77 used protein network associations to examine plausible pathways through which they could
 78 be influencing birth weight. **Figure 1** summarises the analytical workflow used in this paper.



81 **Figure 1** – Schematic representation of the analyses conducted in this paper. Abbreviations:
 82 GWAS, genome wide association studies; pQTL, protein quantitative trait loci

83

84 Selection of genetic instruments for plasma proteins

85 We selected genetic instruments from the deCODE GWAS of plasma proteins, which
 86 provides data on 4,459 unique proteins, mapped to 13,514 pQTL. For our analyses, we
 87 excluded trans instruments (N=2,647 proteins with 6,402 trans pQTL) and secondary
 88 variants (N=5,238 secondary pQTL) retaining 1,783 cis pQTL defined as all those within
 89 $\pm 1 \text{ Mb}$ for 1,812 proteins ($P < 1 \times 10^{-7}$) (**Supplementary Figure 1**)

90 Discovery sample

91

92 We used publicly available meta-analysed GWAS summary data on birth weight. These data
93 were obtained from the 2019 Early Growth Genetics (EGG) consortium plus UK Biobank
94 (UKBB) GWAS. This GWAS has publicly available estimates of maternal genetic
95 associations adjusted for fetal genotype and fetal genetic associations adjusted for maternal
96 genotype (see below 'Adjustment for maternal/offspring genotype').

97 The following exclusions were made prior to running the GWAS: i) twins and other multiple
98 births, ii) offspring born earlier than 37 weeks of gestation, iii) extreme birth weight outliers
99 (only individuals born between 2.2kg and 4.6kg were included in the maternal GWAS, and
100 individuals born between 2.5 and 4.5kg were included in the offspring GWAS) and iv) babies
101 born with congenital anomalies (for the maternal genotype only). Genetic associations with
102 birth weight were reported by the GWAS in standard deviation (SD) units. We multiplied
103 these by 551.36 (the SD of birth weight in the UKB) to obtain results in grams (g).

104 Overall, N=406,063 participants contributed to the models estimating the maternal and fetal
105 genetic effects on birth weight that were adjusted, respectively, for fetal and maternal
106 genotype. These included N=101,541 participants who reported their own birth weight and
107 birth weight of their first child, N=195,815 participants with their own birth weight (fetal
108 GWAS), and N=108,707 female participants with data on offspring birth weight (maternal
109 GWAS)(8) (17).

110 Replication study

111

112 For independent replication, we used genetic association data for birth weight from MoBa, a
113 population-based pregnancy cohort study conducted by the Norwegian Institute of Public
114 Health. Pregnant women and their partners were recruited from all over Norway from 1999-
115 2008. The women consented to participate in 41% of the pregnancies. The cohort includes
116 approximately N=114,500 children, N=95,200 mothers, and N=75,200 fathers (18). The
117 current study uses version 12 of the quality-assured genetic data files released for research
118 in January 2019. Birthweight was obtained from linked clinical records held in Medical Birth
119 Registry of Norway (MBRN, a national health registry established in 1967 that contains
120 information about all births in Norway, which is linked to the MoBa study using unique
121 personal identification numbers). Questionnaire responses from mothers and fathers data
122 were used to identify sex registered at birth, year of birth, birth weight, and multiple births
123 (only available in the offspring). As in the discovery GWAS, multiple births and extremes of
124 birth weight were excluded. Analyses were adjusted for principal components (PCs) and
125 genotyping batch.

126 In MoBa, plasma blood samples were obtained from both parents during pregnancy, and
127 from umbilical cord at birth (19). This project used MoBa genetic data that was quality
128 controlled and imputed using the MoBaPsychGen pipeline, which has previously been
129 described (20). Phasing and imputation were performed using the publicly available
130 Haplotype Reference Consortium release 1.1 panel as a reference (21). The pipeline output
131 consists of best-guess hard-call genotype data for 6,981,748 variants in 207,409 MoBa
132 participants of European ancestry. GWAS in MoBa were run using *regenie* software (v 3.1.2)
133 on the TSD server (22).

134 Adjustment for maternal/offspring genotype

135

136 Birth weight is influenced by both maternal and fetal genotype. Therefore, to distinguish
137 maternal and fetal genetic effects, in the discovery GWAS a weighted linear model was used
138 to estimate maternal genetic associations (adjusted for fetal genotype), and fetal genetic
139 associations adjusted for maternal genotype (3). From this, genetically-instrumented
140 maternal effects of proteins on birth weight (not mediated or biased due to horizontal
141 pleiotropy via fetal effects) and genetically instrumented fetal effects of proteins on birth
142 weight (not confounded by maternal genotype) can be estimated. For our discovery sample
143 (EGG+UKB GWAS), we downloaded these adjusted estimates from the GWAS consortium
144 website. For our replication sample (MoBa), we estimated adjusted associations using the
145 weighted linear model implemented via the DONUTS software package (51). As part of this,
146 we used genetic covariance intercepts from LD score regression (LDSC) to account for
147 overlap between maternal and fetal GWAS sample (23). The summary maternal adjusted for
148 fetal, and fetal adjusted for maternal results were then used in our replication two-sample
149 MR.

150 Two sample MR

151

152 We conducted MR analyses to study the causal effects of circulating maternal and fetal
153 proteins on birth weight. All MR analyses were performed using the *TwoSampleMR* R
154 package version 0.5.6 (26). We used the Wald ratio estimator for analyses as only one pQTL
155 was available per protein. Prior to MR analysis, genetic association data for proteins and
156 birth weight were harmonized so that the effect of each genetic variant on the exposure and
157 outcome were relative to the same effect allele. In some instances, data could not be
158 harmonised (due to being palindromic SNPs, A/T or G/C, with allele frequencies close to
159 50%), and these pQTL and their corresponding proteins were removed from further analyses
160 (**Supplementary Table 2**). After excluding pQTL that failed harmonisation, we retained data
161 for 1,139 proteins instrumented by the same number of *cis* pQTL (**Figure 1** and
162 **Supplementary Figure 1**). We then analysed maternal and fetal data separately. MR results

163 with a FDR-adjusted p-value ≤ 0.05 were carried forward to the replication MR and
164 subsequent analyses.

165 We sought replication of the discovery MR results using genetic association data for birth
166 weight from MoBa participants. There is no overlap between the discovery and replication
167 participants. The same procedures for data harmonisation and two-sample MR analyses
168 described in the discovery stage were used in the replication analyses. To report MR results
169 as the mean difference in birth weight (g) per 1 SD increase in protein level, we multiplied
170 MR effect estimates and standard error by 565.63 (g), which corresponds to 1 SD of birth
171 weight in MoBa. We then conducted a fixed effects meta-analysis of estimates from
172 discovery and replication samples using the *meta* R package (version 6.5-0). Our criteria for
173 replication were: i) directionally consistent results between discovery and replication, ii)
174 associations with a p-value threshold < 0.05 in the meta-analysis, as commonly used in
175 GWAS, and reflecting the relatively modest size of the replication sample in comparison to
176 the main analysis sample and (iii) there was no strong evidence supporting heterogeneity
177 between discovery and replication MR estimates (Cochrane's Q p-value > 0.05).

178 Genetic colocalization

179
180 We undertook genetic colocalization analyses using the *coloc* R package (24) to investigate
181 whether our MR findings were compatible with a shared causal variant or confounded by
182 linkage disequilibrium (LD) (24). This could happen if a selected pQTL is in LD with another
183 genetic variant influencing birth weight via another biological mechanism. *Coloc* computes
184 all possible configurations of causal variants for each of two traits and uses a Bayesian
185 approach to calculate support for each causal model (H_0 : no association; H_1 : association
186 with protein only; H_2 : association with birth weight only; H_3 : both traits owing to distinct
187 causal variants; H_4 : both traits owing to a shared causal variant). We restricted the analyses
188 to a ± 500 kb window around the pQTL, and assumed a prior probability that any pQTL in the
189 region is associated with the protein only (p_1) of 1×10^{-4} , birth weight only (p_2) of 1×10^{-4} , or
190 both traits (p_{12}) 1×10^{-5} . We considered a posterior probability of association (PPA) for $H_4 >$
191 0.70 to provide strong evidence for colocalization, while a PPA for $H_3 > 0.5$ was considered
192 as evidence against colocalization. To facilitate visualisation of genomic signals in each
193 region, we generated stacked recombination plots using the *locuscompareR* R package
194 (<http://locuscompare.com/>) (25).

195 Where available, we extracted genetic association data for the genomic regions selected for
196 colocalization analyses for plasma proteins and birth weight using the IEU Open GWAS
197 (<https://gwas.mrcieu.ac.uk/>). The summary statistics for the genetic associations were
198 downloaded from the deCODE website <https://www.decode.com/summarydata/>.

199 Fetal expression lookup
200

201 One of the assumptions of MR is that the genetic instruments are statistically strongly
202 associated with the phenotype in the population to which inference would be made (i.e. the
203 relevance assumption). We were unable to determine whether our genetic instruments
204 associated with fetal (in utero) circulating proteins, due to the absence of large-scale
205 datasets with both offspring genetic data and cord-blood measures of circulating proteins.
206 Instead, we explored whether the proteins with evidence from discovery and replication were
207 expressed in fetal tissue. We used the single-cell transcriptomics data from the human cell
208 atlas of fetal gene expression (26). The atlas was developed from 121 human fetal samples
209 (post-conceptual age = 72-129 days) from 15 organs (eye, heart, intestine, kidney, liver,
210 lung, muscle, pancreas, placenta, spleen, stomach, thymus, adrenal, cerebellum and
211 cerebrum), profiling 4 million single cells using a sci-RNA-seq3 protocol. The authors used a
212 clustering approach building on a form of principal components analysis (uniform manifold
213 approximation and projection - UMAP) to generate a resource where fetal gene expression
214 can be mapped across different organs, tissues and cell types
215 (<https://descartes.brotmanbaty.org/>). We used this resource to check that our proteins of
216 interest were expressed in fetal tissue, as a further line of evidence.

217

218 Protein networks

219 We explored information on protein-protein associations (referred to as interactions in
220 genetic research) from the STRING database (<https://string-db.org/cgi>) to gain insights into
221 presumed biological processes underlying our findings. STRING collates information from all
222 known protein-protein interactions databases and provides a visual network of predicted
223 associations for a particular group of proteins, whereby the proteins are represented as
224 'nodes' and the lines which join them are the predicted functional associations. The colour of
225 the line denotes the source of the interaction information (see figure legend) (27). We set the
226 confidence score of a given association to be 'high confidence' and restricted to associations
227 from curated databases (either KEGG, Reactome, BioCyc and Gene Ontology, as well as
228 legacy datasets from PID and BioCarta), experimentally determined (where evidence comes
229 from lab experiments), reported from gene fusions (from reported gene fusion events), gene
230 co-occurrence (where gene families have similar occurrence patterns across genomes), co-
231 expression (where gene are shown to be correlated in expression across a large number of
232 datasets) and protein homology (where proteins may have similar structures).

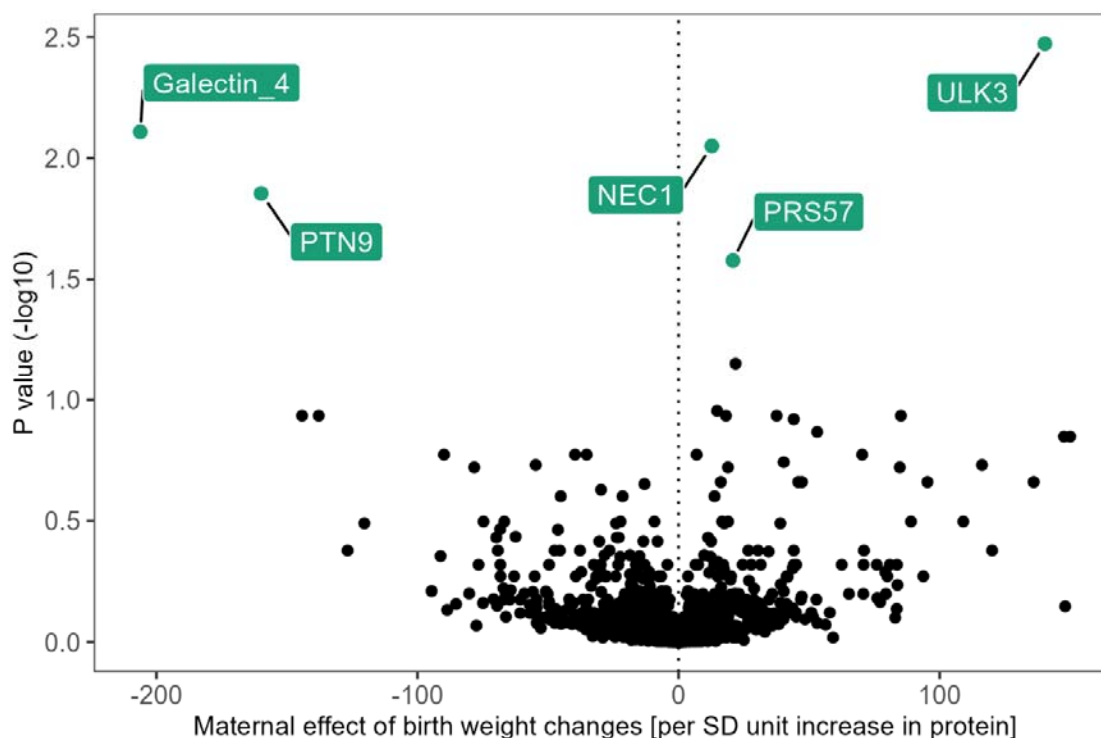
233

234 Results

235 Identifying causal effects of maternal circulating proteins on offspring birth weight

236

237 We found evidence of causal effects of 5 maternal proteins (instrumented by 5 cis-pQTLs)
238 on offspring birth weight that passed our 5% false discovery rate (FDR) adjusted p-value
239 **(Figure 2)**. We found evidence that higher NEC1 increased birth weight (mean-difference:
240 12g (95% CI: 6g, 18g) per 1 standard deviation protein level) as did PRS57 (20g (10g, 31g))
241 and ULK3 (140g (81g, 199g)). Higher maternal levels of Galectin_4 decreased birth weight (-
242 206g (-299g, -113g)), as did PTN9 (-159g (-237g, -82g)). **(Figure 2)**.



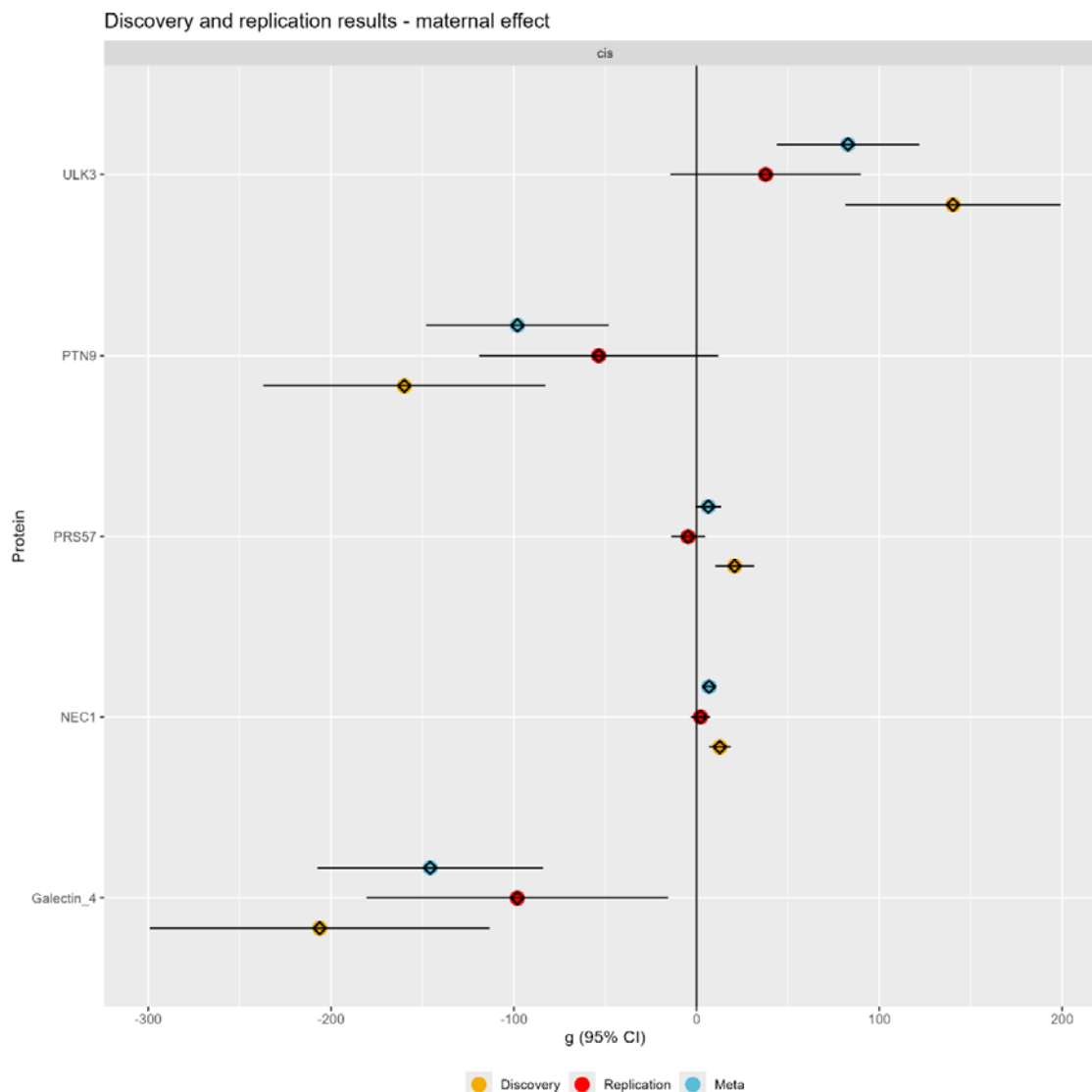
243

244 **Figure 2** – Two sample MR results using maternal cis pQTLs against offspring birth weight.
245 FDR corrected p-values transformed to their $-\log_{10}$. Results plotted in green passed 5%
246 FDR corrected p-value threshold. Abbreviations: SD, standard deviation

247

248 MR results for maternal proteins NEC_1, Galectin_4, ULK3 and PTN9 identified in discovery
249 analyses met our replication criteria based on meta-analysed results from pooled discovery
250 and replication. However, the replication result for PRS57 was not directionally consistent
251 and there was evidence of high heterogeneity in the meta-analysis for PRS57, ULK3, PTN9
252 **(Figure 3 and Supplementary Table 6 and 8)**.

253



254

255 **Figure 3** Mendelian randomization results estimating the effect of genetically instrumented
256 maternal proteins (in standard deviation units) on offspring birth weight (in grams) in the
257 discovery (orange dots N=210,248 mothers), replication (red dots; N=87,651 mothers) and
258 meta-analysed discovery and replication data. Replication was tested for proteins passing
259 FDR-corrected p-value <0.05 in the discovery data. Our criteria for replication were: i)
260 directionally consistent results between discovery and replication, ii) associations with a p-
261 value threshold <0.05 in the meta-analysis, as commonly used in GWAS, and reflecting the
262 relatively modest size of the replication sample in comparison to the main analysis sample
263 and (iii) there was no strong evidence supporting heterogeneity between discovery and
264 replication MR estimates (Cochrane's Q p-value > 0.05).

265

266 For maternal effects, we undertook colocalization analysis for all proteins which passed our
267 FDR-adjusted p-value in the discovery analysis. For colocalization analyses, results are
268 shown in **Table 1** as posterior probabilities (PP) of no association (H_0), association with
269 protein only (H_1), birth weight only (H_2), both traits owing to distinct causal variants (H_3), or

270 both traits owing to a shared causal variant (H_4) (24). The colocalization analyses supported
271 causal effects for maternal circulating NEC1, Galectin_4 and PRS57 with offspring birth
272 weight, with high H_4 of 0.82, 0.84, and 0.76 respectively (**Table 1**). For PTN9 and ULK3,
273 there was strong evidence that the association stemmed from distinct causal variants.

274 **Table 1** – Genetic colocalization results for maternal proteins with birth weight

Protein	H_0	H_1	H_2	H_3	H_4
NEC1	0	0.05	0	0.13	0.82
Galectin_4	0	0.06	0	0.10	0.84
PTN9	0	0	0	0.99	0
ULK3	0	0	0	0.93	0.06
PRS57	0	0.21	0	0.03	0.76

275 Abbreviations – PP, posterior probabilities; H, hypothesis. Results are expressed as
276 posterior probabilities (PP) of no association (H_0), association with protein only (H_1), birth
277 weight only (H_2), both traits owing to distinct causal variants (H_3), or both traits owing to a
278 shared causal variant (H_4).

279 Maternal discovery and replication MR, and colocalization results of are summarised in
280 **Table 2**. Together these provide strong evidence for maternal circulating proteins Galectin_4
281 and NEC1 being identified in discovery, replication, and not being biased due to confounded
282 by LD (H_4 0.84 and 0.82, respectively). There was statistical support for PRS57 in the
283 discovery and colocalization analysis (H_4 0.76), but not the replication. Whilst there was
284 good replication for ULK3, colocalization results for ULK3 and PTN9 suggested results were
285 being driven by distinct causal variants ($H_3 > 0.9$).

286

287

288

289

290

291

292

293

294

295 **Table 2** – Summary of results from analyses exploring the effect of maternal proteins on
 296 offspring birth weight

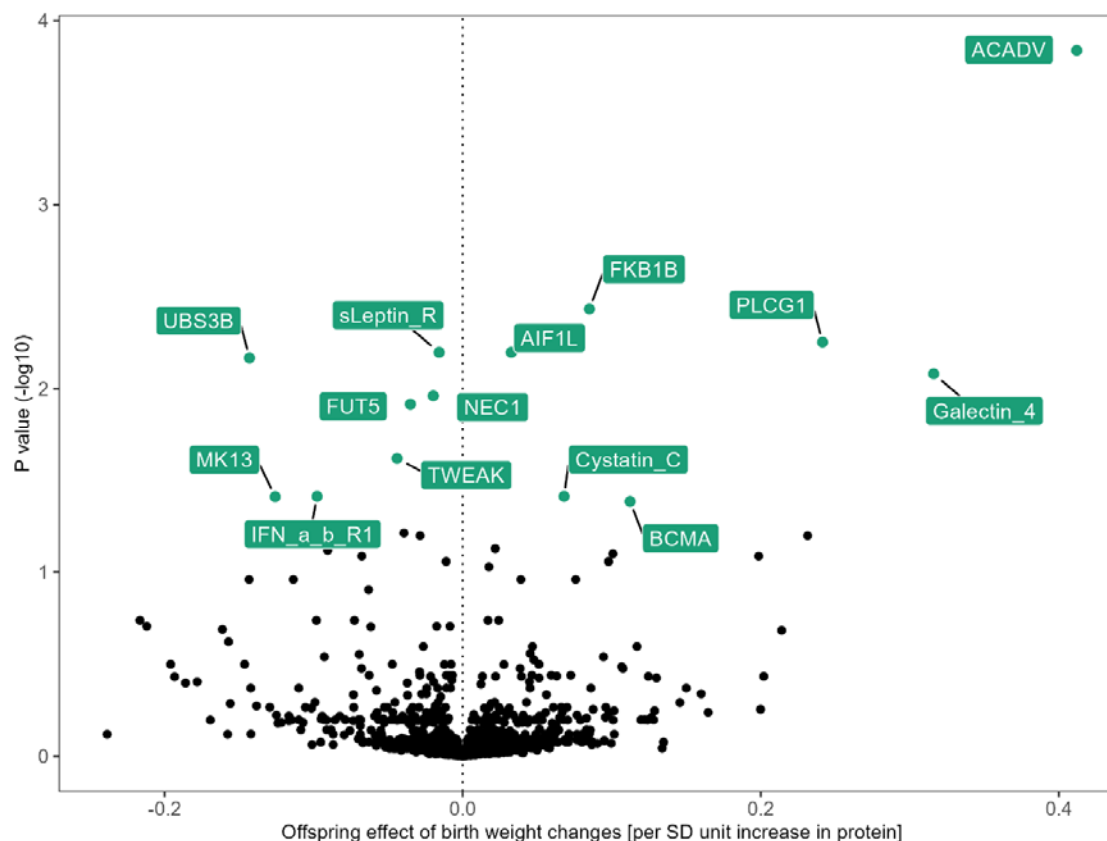
Protein	Uniprot ID	Discovery MR direction of effect	Independently replicated	Colocalization
NEC1	P29120	+	Yes	Yes
Galectin_4	P56470	-	Yes	Yes
PTN9	Q99952	-	Yes	No
ULK3	Q6PHR2	+	Yes	No
PRS57	Q6UWY2	+	No	Yes

297

298 Identifying causal effects of fetal circulating proteins on offspring birth weight

299

300 We found evidence of causal effects of 14 proteins on offspring birth weight. Higher
 301 genetically-predicted offspring levels of NEC1 decreased birth weight (-10g (-16g, -5g),
 302 alongside sLeptin_R (-8g (-12g, -4g)), UBS3B (-78g (-116g, -41g)), FUT5 (-19g (-29g, -9g)),
 303 IFN_a_b_R1 (-53g (-84g, -23g)), TWEAK (-24g, (-37g, -11g)) and MK13 (-69g (-108g, -
 304 30g)). Higher fetal levels of Galectin_4 increased birth weight (174g (89g, 258g)), alongside
 305 ACADV (227g (142g, 311g)), PLCG1 (133g (72g, 193g)), BCMA (61g (27g, 96g)) Cystatin C
 306 (37g (16g, 58g), and FKB1B (46g (26g, 67g)) (**Figure 4**).

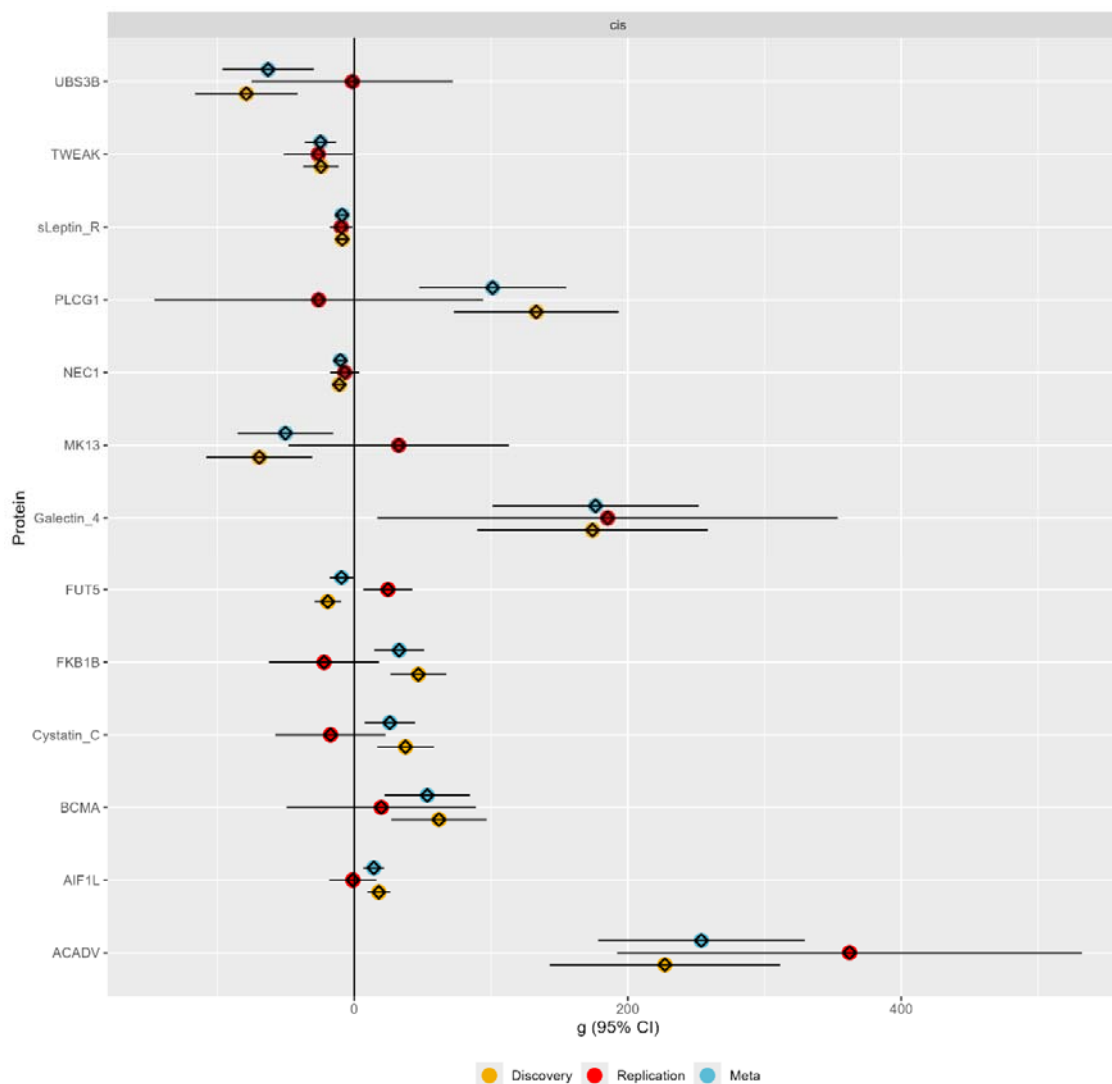


307

308 **Figure 4** – Fetal two sample MR results for cis pQTL. FDR corrected p-values transformed
309 to their $-\log_{10}$. Results plotted in green passed FDR corrected p-value threshold.
310 Abbreviations: SD, standard deviation

311

312 As in the maternal effects analysis, we conducted replication in MoBa and then ran a meta-
313 analysis. We found meta-analysed MR results consistent with discovery for NEC1,
314 Galectin_4, sLeptin_R, TWEAK, ACADV, UBS3B, BCMA (same direction of effect and with a
315 meta-analysed FDR adjusted pvalue <0.05 and no evidence of between discovery and
316 replication results heterogeneity). PLCG1, MK13, FUT5, FKB1B, and Cystatin_c did not
317 replicate, and the replication sample estimate had the opposite direction of effect to the
318 discovery sample (**Figure 5** and **Supplementary Table 7**). The pQTL for protein
319 IFN_a_b_R1 was not in our replication data so could not be tested or meta-analysed
320 (**Supplementary Table 9**).



321

322 **Figure 5** Mendelian randomization analyses estimating the effect of genetically-instrumented
 323 fetal proteins (in standard deviation units) on offspring birth weight (in grams) in the
 324 discovery (N=297,356 offspring, orange dots), replication (N=62,108 offspring, red dots) and
 325 meta-analyses (blue dots) of discovery and replication samples. Replication was tested for
 326 proteins passing FDR-corrected p-value <0.05 in the discovery data. Our criteria for
 327 replication were: i) directionally consistent results between discovery and replication, ii)
 328 associations with a p-value threshold <0.05 in the meta-analysis, as commonly used in
 329 GWAS, and reflecting the relatively modest size of the replication sample in comparison to
 330 the main analysis sample and (iii) there was no strong evidence supporting heterogeneity
 331 between discovery and replication MR estimates (Cochrane's Q p-value > 0.05).

332

333 For fetal effects, we undertook colocalization analysis for all proteins which passed our FDR
 334 adjusted p-value in the discovery analysis. There was strong evidence of colocalization for
 335 NEC1, ACADV, PLCG1, FUT5, IFN_a_b_R1, AIF1L and UBS3B (all $H_4 > 0.75$). There was
 336 moderate evidence of colocalization for sLeptin_R (H_4 0.65). There was evidence that the
 337 MR results for fetal Galectin_4, Cystatin-C, BCMA and MK13 might be explained by LD
 338 confounding ($H_3 > 0.5$ or high H_1) (**Table 3**).

339 **Table 3** – Genetic colocalization results for offspring proteins with birth weight.

Protein	H ₀	H ₁	H ₂	H ₃	H ₄
NEC1	0	0.14	0	0.09	0.77
Galectin_4	0	0.07	0	0.57	0.35
ACADV	0	0	0	0.16	0.83
CystatinC	0	0.42	0	0.08	0.49
BCMA	0	0.45	0	0.09	0.45
TWEAK	0	0	0.6	0.37	0
FUT5	0	0.09	0	0.01	0.88
FKB1B	0	0	0	0.99	0
PLCG1	0	0.03	0	0.09	0.86
MK13	0	0.33	0	0.3	0.37
IFN_a_b_R1	0	0.1	0	0	0.89
AIF1L	0	0.07	0	0	0.93
UBS3B	0	0.05	0	0.01	0.92
sLeptin_R	0	0.03	0	0.3	0.65

340 Abbreviations – PP, posterior probabilities; H, hypothesis. Results are expressed as
 341 posterior probabilities (PP) of no association (H₀), association with protein only (H₁), birth
 342 weight only (H₂), both traits owing to distinct causal variants (H₃), or both traits owing to a
 343 shared causal variant (H₄).

344

345 Fetal discovery and replication MR, and colocalization results of are summarised in **Table 4**.
346 Together these provide strong evidence for fetal circulating proteins.

347

Protein	Uniprot ID	Discovery MR direction of effect	Independently replicated	Colocalization
NEC1	P29120	-	Yes	Yes
Galectin_4	O00214	+	Yes	No
ACADV	P49748	+	Yes	Yes
CystatinC	P01034	+	No	No
BCMA	Q02223	+	No	No
TWEAK	O43508	-	Yes	No
FUT5	Q11128	-	No	Yes
FKB1B	Q96AY3	+	No	No
PLCG1	P19174	+	No	Yes
MK13	Q92910	-	No	No
IFN_a_b_R1	P14787	-	NA	Yes
AIF1L	Q9H8A1	+	No	Yes
UBS3B	Q8WUW0	-	Yes	Yes
sLeptin_R	P48357	-	Yes	Uncertain

348

349 Fetal expression lookup

350

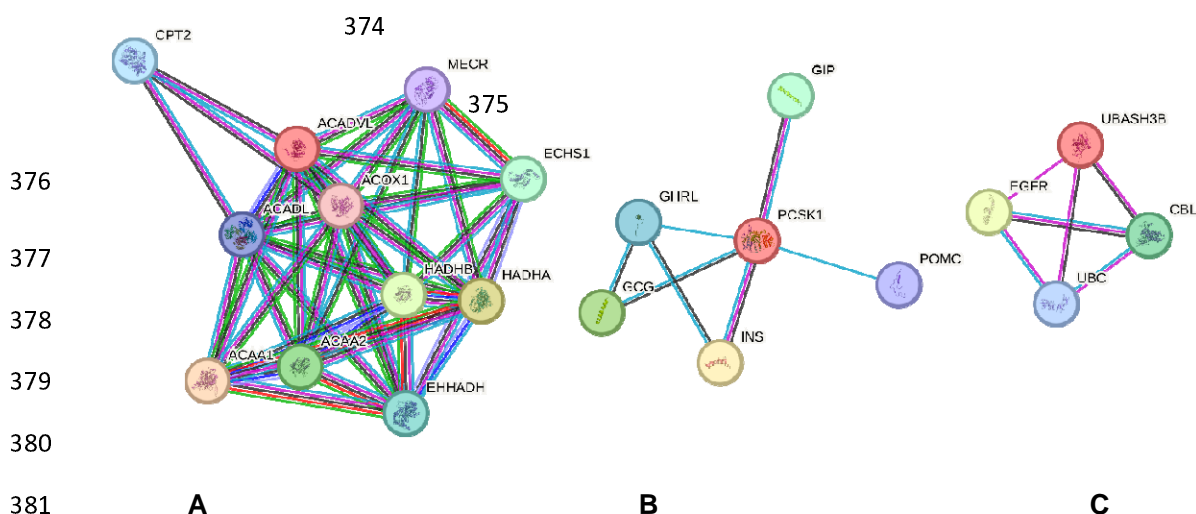
351 As a sanity check of our fetal results, we were able to check whether these genes are
352 expressed in fetal tissue using an atlas of human gene expression during development
353 (<https://descartes.brotmanbaty.org/>). We wanted to see if tissue expression data supported
354 expression of the proteins with evidence from discovery and replication or colocalization in
355 fetal tissue. We found this was the case for genes encoding NEC1 (in pancreas), FUT5 (in
356 lung and thymus), Galectin_4, UBS3B, sLeptin_R, AIF1L, PLCG1, IFN_a_b_R1 and ACADV
357 (all expression all across multiple tissues) (**Supplementary Figures 20-29**).

358 Protein networks of identified maternal and fetal proteins affecting birth weight

359 We undertook protein-protein association analyses for the proteins that replicated in the MR
360 results, and had supporting colocalization results in either maternal (NEC1, Galectin_4) or
361 fetal analyses (NEC1, ACADV, UBSH3B).

362 We found evidence that NEC1 (proprotein convertase 1, the same enzyme as PCSK1, as in
363 the **Figure 6B** below) associates with proteins regulating glucose homeostasis, such as

364 insulin (INS), and glucagon (GCG) - hormones produced by the pancreas to regulate blood
365 sugar levels. NEC1 is a stimulator of INS (28, 29). It also associates with proteins regulating
366 food intake, such as pro-opiomelanocortin (POMC) and ghrelin (GHRL) (28-31) (**Figure 6B**).
367 UBS3B associated with EGFR (part of the epidermal growth factor family), CBL (critical for
368 cell signalling pathways), and UBC (which helps regulate cell stress) (**Figure 6C**). ACADV
369 had the largest network of associations, including many proteins associated with fatty acid
370 metabolism (ACOX1, CPT2, and other proteins within the thiolase family (enzymes which
371 break down fatty acids) ACAA1 and ACAA2) (**Figure 6A**). However, Galectin_4 and PRS57
372 had no protein networks which survived our criteria (high confidence, and from sources
373 detailed in **Figure 6** footnote).



382 **Figure 6** - Protein-protein associations - proteins with evidence from both discovery,
383 replication, and colocalization analyses. Different line colours represent different sources of
384 evidence for these predictions – known associations from curated databases (light blue) and
385 experimentally determined (pink); predicted associations from gene neighbourhood (green),
386 gene fusions (red), gene co-occurrence (dark blue), co-expression, and protein homology
387 (lilac). Associations are for proteins jointly contributing to a shared function, rather than
388 specifically binding to each other. Splice isoforms or post-translational modifications are
389 collapsed, i.e. each node represents all the proteins produced by a single, protein-coding
390 gene locus. The physical distances between two nodes along an edge in a graph have no
391 meaning.

392 Discussion

393 We have used two-sample MR to explore the causal effect of maternal pregnancy and fetal
394 plasma proteins on offspring birth weight. We found evidence of potential causal effects,
395 unlikely to be explained by chance or confounding by LD, for 2 maternal circulating proteins
396 (NEC1, Galectin_4) and 3 fetal circulating proteins (NEC1, ACADV, and UBS3B). For the
397 remainder of the discussion, we focus mainly on these proteins which had the strongest
398 evidence across all analyses.

399 Proteins with opposing maternal and fetal effects on birthweight

400 Two proteins, NEC1 and Galectin_4, instrumented by cis-pQTLs, appear to be acting in
401 opposite directions when comparing maternal and fetal MR results. They suggest that more
402 NEC1 from the mother leads to higher birth weight, yet more NEC1 from the fetus leads to
403 lower birth weight – as in the case with insulin and other regulators of fetal growth. This is
404 consistent with previous work showing the role of NEC1 in regulating proinsulin processing
405 (32). Indeed, a new drug (Setmelanotide) being tested to treat obesity is known to perturb
406 PCSK1, because PCSK1 mutations lead to deficient signalling in melanocortin pathways
407 (e.g. because of a lack of α -MSH). Setmelanotide activates MC4R to restore appetite
408 control, addressing genetic obesity caused by disrupted PCSK1 function (33). This is further
409 evidence that our findings could represent molecular targets for birth weight. The STRING
410 protein-protein associations in this study show this link between NEC1 and insulin (INS) and
411 glucagon (GCG) (**Figure 6B**), demonstrating this known function in glucose homeostasis. It
412 is important to note that whilst these protein-protein associations show co-expression (which
413 may be downstream of a certain mechanism), they do not always imply interaction.
414 Furthermore, the different sources of evidence are important when interpreting these
415 interaction networks. We did not include text-mining and gene neighborhood interactions in
416 the STRING networks so we could follow the most robust lines of evidence, and set a high
417 confidence threshold. This may explain why we did not identify any associations for some
418 proteins that replicated and were supported by colocalization, or because proteins like
419 Galectin_4 are poorly characterized (27).

420 In our analysis, Galectin_4 was shown to the opposite direction of effect to NEC1 on birth
421 weight. More Galectin_4 from the mother leads to lower birthweight and more Galectin_4
422 from the fetus leads to higher birthweight. Galectin_4 is part of the Galectin family which
423 binds carbohydrates, lactose and sugars (34). Previous work has shown that the Galectin
424 family of β -galactoside binding proteins are important in modulating diverse developmental
425 processes. They contribute to placentation and regulate maternal immune tolerance (34) and
426 have been previously suggested as biomarkers for adverse pregnancy outcomes like
427 gestational diabetes (35) and infertility (34). Other expression studies have shown the
428 importance of Galectins in pregnancy, and the importance of a maternal-fetal balancing act
429 for ideal pregnancy outcomes. For example, lower levels of fetal expression of Galectins 3, 8
430 and 9 have previously been associated with intrauterine growth restriction (34). However,
431 most of the previous studies of plasma Galectin_4 concentrations in pregnancy have come
432 from mouse or in vitro models (35). It has not been well characterised either inside or outside
433 of pregnancy, demonstrated by the lack of reported associations from the protein-protein

434 association models. Our study provides an additional line of evidence of a potential role of
435 Galectin_4 in fetal growth however there was a lack of colocalization in the fetal effects
436 analysis (34).

437 PRS57 had strong evidence in the discovery and colocalization analyses for increasing birth
438 weight, however it was the only protein in the maternal analyses which did not replicate.
439 Whilst other members of the serine protease family (a large family of protein-cleaving
440 enzymes) appear critical in pregnancy (e.g. high levels of other serine protease proteins are
441 associated with preeclampsia (36)), to our knowledge, PRS57 has not been previously
442 linked with birth weight, or other disorders of pregnancy. In contrast, PTN9 and ULK3 had
443 evidence from discovery and replication, but not from colocalization. Unfortunately, we had
444 limited power to explore further bias in MR results due to confounding by LD, but high H_3
445 results suggest this was down to the traits not sharing the same causal variant, although it
446 could also be related to violations of coloc's assumptions due to multiple causal variants.

447 Proteins with fetal-specific effects on birthweight

448 UBS3B and ACADV had good evidence from discovery, replication, and colocalization. In
449 our analysis, we found higher UBS3B lowered birth weight. UBS3B is a protein that is not yet
450 well characterised for its role in pregnancy, but known to be associated with cellular
451 processes for mammalian development (37). ACADV (very long-chain acyl-coenzyme A
452 dehydrogenase, also known as VCLAD) catalyses the first step in beta-oxidation of long-
453 chain fatty acids to release energy (38).

454 In our fetal analysis, we found evidence that higher fetal cis-pQTL instrumented sLeptin_R
455 reduced birth weight. sLeptin_R has a well-established role in energy metabolism, body
456 weight, and is secreted in fetal tissue and the placenta (39). The strong birth weight-
457 associated locus near *CCNL1* from previous GWAS is also associated with leptin levels in
458 adults, providing orthogonal evidence for a key role of this signalling pathway in fetal growth
459 (40). There was good evidence for replication in our study, however the colocalization results
460 fell slightly short of our threshold (H_4 0.65, as opposed to 0.70).

461 Strengths and limitations

462 We have integrated the largest-scale proteomics and birthweight genetic association data to
463 shed light on maternal and fetal molecular mechanisms regulating fetal growth. Furthermore,
464 we have used large scale birth weight data from three large European cohorts (EGG, UK
465 Biobank and MoBa) for our discovery, replication analyses and meta analyses. We have

466 undertaken sensitivity analyses, including checking for confounding by LD and attempted to
467 further explain the underlying biology of our molecular findings.

468 In terms of limitations, our analysis has a limited coverage of the proteome due to the use of
469 GWAS data on plasma proteins. For example, because they are not covered in existing
470 proteomic GWAS, we were unable to assess the effects of two key placental expressed
471 proteins - sFlt-1 and PlGF - , which have biological support for affecting fetal growth, and
472 are now used clinically to predict risk of fetal growth restriction and pre-eclampsia in many
473 countries (41-43). To explore effects of these and potentially other placental proteins we
474 would need large proteomic GWAS of maternal pregnancy and cord-blood proteins. It is also
475 likely that there are additional causal proteins that are not placental-/pregnancy-specific,
476 which might be identified in future, where studies have access to even larger proteomics
477 panels, or using cell- or tissue-specific proteomics.

478 Another potential limitation is related to epitope effects intrinsic to the proteomic technology.
479 Whilst we aimed to reduce the likelihood of misclassification of protein levels through epitope
480 effects (i.e. differences in antigen recognition, rather than protein levels) we cannot rule out
481 some bias from these effects (44). We removed trans-pQTL and only retained cis-pQTL due
482 to the higher possibility of bias due to pleiotropic mechanisms (45). For each protein we only
483 had one SNP, so methods that have been developed to explore bias due to horizontal
484 pleiotropy are not possible.

485 In using population level proteomics data, a further limitation is that in the exposure data,
486 whilst we can assume in the maternal analysis that the offspring proteins won't affect the
487 levels of the maternal proteins, in the offspring analysis, the assumption that maternal
488 proteins won't affect offspring proteins may not hold. However, there is no way to directly
489 test this.

490 Furthermore, we have assumed that genetic variants identified in protein GWAS conducted
491 in males and non-pregnant women are similarly associated with circulating proteins in
492 fetuses and pregnant women. Ideally, we would test this in studies that have GWAS data
493 and circulating protein levels in women during pregnancy and cord-blood. However, such
494 data is not currently available or only available in small numbers (for example, there is
495 protein data profiled during pregnancy in the Born in Bradford (BiB) cohort, however the
496 Olink coverage is fewer than 453 proteins in 4000 women, with none of these proteins
497 overlapping with our top hits). However we found evidence that some of the proteins (i.e.
498 NEC1, Galectin_4) that our MR results suggest affect birth weight, are expressed in fetal
499 tissue, which provides some support for their relevance to pregnancy and fetal intrauterine

500 mechanisms. Additionally, supporting evidence from other studies, where genetic variants
501 are instrumental variables for social, behavioural, and molecular exposures during
502 pregnancy, reveals consistent associations with those identified in GWAS of both women
503 and men. This suggests that the assumption is unlikely to be violated. Significantly, with
504 respect to this paper, we have previously demonstrated that among 89 associations
505 involving genetic instruments for one or more of 9 amino acids, there was substantial
506 consistency between those GWAS results derived in men and non-pregnant women, to
507 outcomes in women only (46). This consistency was also observed in women who were
508 pregnant at the time of amino acid measurement for 67 out of the 89 associations (75%). In
509 the remaining 22 associations where heterogeneity was evident, it was likely attributed to the
510 poor quality of genetic imputation for certain variants in the pregnancy study (46).

511 Conclusions

512 We found strong evidence for causal effects of several proteins on offspring birth weight
513 across a range of analyses, highlighting proteins with opposing maternal and offspring
514 effects (NEC1, Galectin_4), and fetal (sLeptin_R, UBS3B, ACADV) effects. These proteins
515 are involved in multiple biological processes governing glucose homeostasis, energy
516 metabolism, endothelial function and adipocyte differentiation. These findings provide new
517 insights into maternal and fetal molecular mechanisms regulating fetal growth.

518 **Abbreviations**

519 EGG: Early Growth Genetics consortium

520 eQTL: expression quantitative trait loci

521 GWAS: genome-wide association study

522 LD: linkage disequilibrium

523 MoBa: Norwegian Mother, Father and Child Cohort Study

524 MR: Mendelian Randomisation

525 PP: predicted probability

526 pQTL: protein quantitative trait loci

527 SNP: single nucleotide polymorphism

528 UKBB: UK Biobank

529 **Declarations**

530 **Ethics approval and consent to participate**

531 All human research was approved by the relevant institutional review boards and conducted
532 according to the Declaration of Helsinki. Participants of all studies in the Early Growth
533 Genetics (EGG) consortium provided written informed consent. The UK Biobank has
534 approval from the North West Multi-Centre Research Ethics Committee, which covers the
535 United Kingdom. The establishment of the Norwegian Mother Father and Child (MoBa) birth
536 cohort and initial data collection was based on a license from the Norwegian Data Protection
537 Agency and approval from The Regional Committees for Medical and Health Research
538 Ethics. The MoBa cohort is currently regulated by the Norwegian Health Registry Act. The
539 current study was approved by The Regional Committees for Medical and Health Research
540 Ethics (223273).

541 Consent for publication

542 NA

543 **Availability of data and materials**

544 **Data availability**

545 Data on birth weight in our discovery analysis was contributed by the EGG Consortium using
546 the UK Biobank Resource and was downloaded from www.egg-consortium.org. The
547 genotype and phenotype data are available on application from the UK Biobank
548 (<http://www.ukbiobank.ac.uk/>). Individual cohorts participating in the EGG Consortium should
549 be contacted directly as each cohort has different data access policies. The exposure
550 summary data from which genetic instruments were selected for pQTL are available from
551 EpiGraphDB pQTL browser (<https://epigraphdb.org/pqtl>). Data from MoBa are available from
552 the Norwegian Institute of Public Health after application to the MoBa Scientific Management
553 Group (see its website [https://www.fhi.no/en/op/data-access-from-health-registries-health-
554 studies-and-biobanks/data-access/applying-for-access-to-data/](https://www.fhi.no/en/op/data-access-from-health-registries-health-studies-and-biobanks/data-access/applying-for-access-to-data/) for details).

555 **Acknowledgments**

556 We gratefully acknowledge the participants in the studies, who were directly or indirectly
557 participating, via consortia summary data, contributed to this research. We also are grateful
558 to researchers who made their data open access. The Norwegian Mother, Father and Child

559 Cohort Study is supported by the Norwegian Ministry of Health and Care Services and the
560 Ministry of Education and Research. We are grateful to all the participating families in
561 Norway who take part in this on-going cohort study. We thank the Norwegian Institute of
562 Public Health (NIPH) for generating high-quality genomic data. This research is part of the
563 HARVEST collaboration, supported by the Research Council of Norway (#229624). We also
564 thank the NORMENT Centre for providing genotype data, funded by the Research Council of
565 Norway (#223273), South East Norway Health Authorities and Stiftelsen Kristian Gerhard
566 Jebsen. We further thank the Center for Diabetes Research, the University of Bergen for
567 providing genotype data and performing quality control and imputation of the data funded by
568 the ERC AdG project SELECTIONPREDISPOSED, Stiftelsen Kristian Gerhard Jebsen, Trond
569 Mohn Foundation, the Research Council of Norway, the Novo Nordisk Foundation, the
570 University of Bergen, and the Western Norway Health Authorities. This work was carried out
571 using the computational facilities of the Advanced Computing Research Centre, University of
572 Bristol - <http://www.bristol.ac.uk/acrc/> and the TSD (Tjeneste for Sensitive Data) facilities,
573 owned by the University of Oslo, operated and developed by the TSD service group at the
574 University of Oslo, IT Department (USIT) (tsd-drift@usit.uio.no). The computations on this
575 platform were performed on resources provided by Sigma2 - the National Infrastructure for
576 High-Performance Computing and Data Storage in Norway.

577 **Funding**

578 This work was supported by the University of Bristol and UK Medical Research Council (
579 MC_UU_00032/05), the US National Institute for Health (R01 DK10324), the European
580 Research Council via Advanced Grant 101021566, the British Heart Foundation
581 (AA/18/7/34219 and CS/16/4/32482) and the National Institute of Health Research Bristol
582 Biomedical Research Centre at University Hospitals Bristol NHS Foundation Trust and the
583 University of Bristol.

584 RMF and RNB were funded by a Wellcome Trust and Royal Society Sir Henry Dale
585 Fellowship (WT104150). RMF is supported by a Wellcome Senior Research Fellowship
586 (WT220390). This research was supported by the National Institute for Health and Care
587 Research Exeter Biomedical Research Centre. This research was funded in part by the
588 Wellcome Trust [WT220390]. J.Z. is supported by grants from the National Key Research
589 and Development Program of China (2022YFC2505203). MCB is funded by a University of
590 Bristol Vice Chancellor's Fellowship. EC is supported by funding from the Research Council
591 of Norway (#274611) and the South-Eastern Norway Regional Health Authority (#2021045).

592 The views expressed in this paper are those of the authors and not necessarily those of the
593 any of the funders listed above.

594 For open access, the authors have applied a CC BY public copyright licence to any Author
595 Accepted Manuscript version arising from this submission.

596 **Author contributions**

597 Study conception: DAL, MCB, RMF; Analysis: NM, MCB; Manuscript drafting: NM;
598 Manuscript revisions: NM, MCB, DAL, AFS, MA, RB, RMF, TB, TRG, JZ, DE, DH, GC, EC,
599 MM

600 **Conflict of interest**

601 The authors report no conflict of interest.

602 **Code availability**

603 All code is available on the GitHub repo <https://github.com/MRCIEU/MR-PREG>

604 **References**

- 605 1. Küpers LK, Monnereau C, Sharp GC, Yousefi P, Salas LA, Ghantous A, et al. Meta-analysis of
606 epigenome-wide association studies in neonates reveals widespread differential DNA methylation
607 associated with birthweight. *Nature Communications*. 2019;10(1):1893.
- 608 2. Leite DFB, Cecatti JG. Fetal Growth Restriction Prediction: How to Move beyond. *The*
609 *Scientific World Journal*. 2019;2019:1519048.
- 610 3. Warrington NM, Freathy RM, Neale MC, Evans DM. Using structural equation modelling to
611 jointly estimate maternal and fetal effects on birthweight in the UK Biobank. *International Journal of*
612 *Epidemiology*. 2018;47(4):1229-41.
- 613 4. Wilcox AJ. On the importance—and the unimportance— of birthweight. *International*
614 *Journal of Epidemiology*. 2001;30(6):1233-41.
- 615 5. Barry CA-O, Lawlor DA, Shapland CA-O, Sanderson E, Borges MA-O. Using Mendelian
616 Randomisation to Prioritise Candidate Maternal Metabolic Traits Influencing Offspring Birthweight.
617 LID - 10.3390/metabo12060537 [doi] LID - 537. (2218-1989 (Print)).
- 618 6. Bond TA, Karhunen V, Wielscher M, Auvinen J, Männikkö M, Keinänen-Kiukaanniemi S, et al.
619 Exploring the role of genetic confounding in the association between maternal and offspring body
620 mass index: evidence from three birth cohorts. *International Journal of Epidemiology*.
621 2019;49(1):233-43.
- 622 7. Iliodromiti S, Mackay DF, Smith GCS, Pell JP, Sattar N, Lawlor DA, et al. Customised and
623 Noncustomised Birth Weight Centiles and Prediction of Stillbirth and Infant Mortality and Morbidity:
624 A Cohort Study of 979,912 Term Singleton Pregnancies in Scotland. *PLOS Medicine*.
625 2017;14(1):e1002228.
- 626 8. Warrington NM, Beaumont RN, Horikoshi M, Day FR, Helgeland Ø, Laurin C, et al. Maternal
627 and fetal genetic effects on birth weight and their relevance to cardio-metabolic risk factors. *Nature*
628 *genetics*. 2019;51(5):804-14.

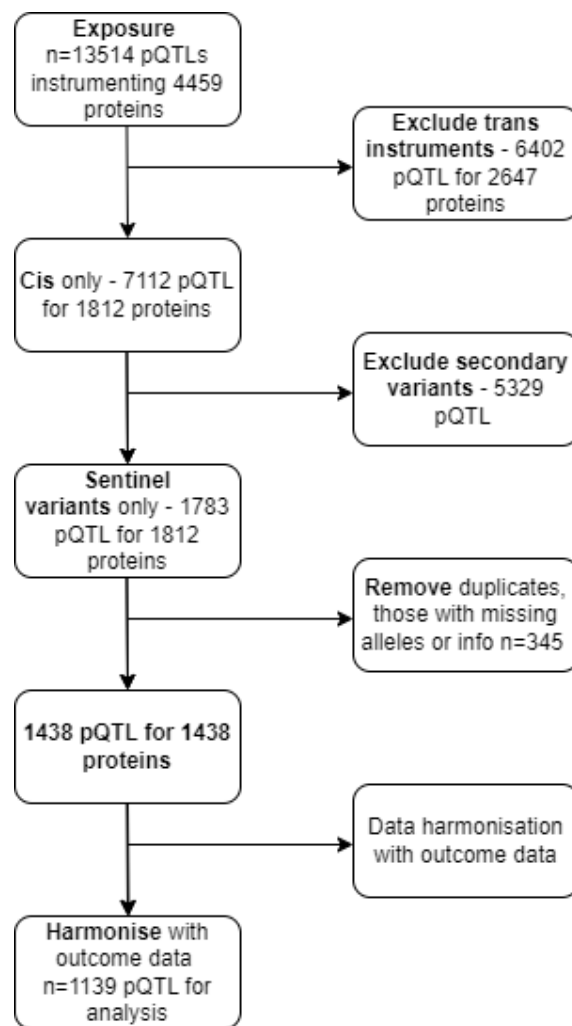
- 629 9. Beaumont RN, Warrington NM, Cavadino A, Tyrrell J, Nodzinski M, Horikoshi M, et al.
630 Genome-wide association study of offspring birth weight in 86,577 women identifies five novel loci
631 and highlights maternal genetic effects that are independent of fetal genetics. (1460-2083
632 (Electronic)).
- 633 10. Ferkingstad E, Sulem P, Atlason BA, Sveinbjornsson G, Magnusson MI, Styrismiddottir EL, et al.
634 Large-scale integration of the plasma proteome with genetics and disease. *Nature Genetics*.
635 2021;53(12):1712-21.
- 636 11. Zheng J, Haberland V, Baird D, Walker V, Haycock PC, Hurle MR, et al. Phenome-wide
637 Mendelian randomization mapping the influence of the plasma proteome on complex diseases.
638 *Nature Genetics*. 2020;52(10):1122-31.
- 639 12. Zhang G, Bacelis J, Lengyel C, Teramo K, Hallman M, Helgeland Ø, et al. Assessing the Causal
640 Relationship of Maternal Height on Birth Size and Gestational Age at Birth: A Mendelian
641 Randomization Analysis. (1549-1676 (Electronic)).
- 642 13. Tyrrell J, Richmond RC, Palmer TM, Feenstra B, Rangarajan J, Metrustry S, et al. Genetic
643 Evidence for Causal Relationships Between Maternal Obesity-Related Traits and Birth Weight. (1538-
644 3598 (Electronic)).
- 645 14. Ardissino MA-O, Slob EA-O, Millar O, Reddy RA-OX, Lazzari L, Patel KHK, et al. Maternal
646 Hypertension Increases Risk of Preeclampsia and Low Fetal Birthweight: Genetic Evidence From a
647 Mendelian Randomization Study. (1524-4563 (Electronic)).
- 648 15. Brand JA-O, Gaillard RA-O, West JA-O, McEachan RA-O, Wright JA-O, Voerman E, et al.
649 Associations of maternal quitting, reducing, and continuing smoking during pregnancy with
650 longitudinal fetal growth: Findings from Mendelian randomization and parental negative control
651 studies. (1549-1676 (Electronic)).
- 652 16. Thompson WA-O, Beaumont RA-O, Kuang AA-O, Warrington NA-OX, Ji Y, Tyrrell JA-O, et al.
653 Higher maternal adiposity reduces offspring birthweight if associated with a metabolically
654 favourable profile. (1432-0428 (Electronic)).
- 655 17. Allen NE, Sudlow C, Peakman T, Collins R, Biobank UK. UK biobank data: come and get it. *Sci*
656 *Transl Med*. 6. United States 2014. p. 224ed4.
- 657 18. Haugan A, Birke C, Alsaker E, Høiseth G, Knudsen GP, Tambs K, et al. Cohort Profile Update:
658 The Norwegian Mother and Child Cohort Study (MoBa). *International Journal of Epidemiology*.
659 2016;45(2):382-8.
- 660 19. Paltiel L, Anita H, Skjerden T, Harbak K, Bækken S, Nina Kristin S, et al. The biobank of the
661 Norwegian Mother and Child Cohort Study – present status. *Norsk Epidemiologi*. 2014;24(1-2).
- 662 20. Corfield EC, Frei O, Shadrin AA, Rahman Z, Lin A, Athanasiu L, et al. The Norwegian Mother,
663 Father, and Child cohort study (MoBa) genotyping data resource: MoBaPsychGen pipeline v.1.
664 *bioRxiv*. 2022:2022.06.23.496289.
- 665 21. McCarthy S, Das S, Kretzschmar W, Delaneau O, Wood AR, Teumer A, et al. A reference
666 panel of 64,976 haplotypes for genotype imputation. *Nature Genetics*. 2016;48(10):1279-83.
- 667 22. Mbatchou J, Barnard L, Backman J, Marcketta A, Kosmicki JA, Ziyatdinov A, et al.
668 Computationally efficient whole-genome regression for quantitative and binary traits. *Nature*
669 *Genetics*. 2021;53(7):1097-103.
- 670 23. Bulik-Sullivan BK, Loh P-R, Finucane HK, Ripke S, Yang J, Patterson N, et al. LD Score
671 regression distinguishes confounding from polygenicity in genome-wide association studies. *Nature*
672 *Genetics*. 2015;47(3):291-5.
- 673 24. Wallace C. Statistical Testing of Shared Genetic Control for Potentially Related Traits. *Genetic*
674 *Epidemiology*. 2013;37(8):802-13.
- 675 25. Liu B, Gludemans MJ, Rao AS, Ingelsson E, Montgomery SB. Abundant associations with
676 gene expression complicate GWAS follow-up. *Nature Genetics*. 2019;51(5):768-9.
- 677 26. Cao J, O'Day DR, Pliner HA, Kingsley PD, Deng M, Daza RM, et al. A human cell atlas of fetal
678 gene expression. *Science*. 2020;370(6518):eaba7721.

- 679 27. Szklarczyk D, Franceschini A, Wyder S, Forslund K, Heller D, Huerta-Cepas J, et al. STRING
680 v10: protein–protein interaction networks, integrated over the tree of life. *Nucleic Acids Research*.
681 2014;43(D1):D447-D52.
- 682 28. Benzinou M, Creemers Jw Fau - Choquet H, Choquet H Fau - Lobbens S, Lobbens S Fau - Dina
683 C, Dina C Fau - Durand E, Durand E Fau - Guerardel A, et al. Common nonsynonymous variants in
684 PCSK1 confer risk of obesity. (1546-1718 (Electronic)).
- 685 29. Stijnen P, Ramos-Molina B, O'Rahilly S, Creemers JWM. PCSK1 Mutations and Human
686 Endocrinopathies: From Obesity to Gastrointestinal Disorders. *Endocrine Reviews*. 2016;37(4):347-
687 71.
- 688 30. Wei X, Ma X, Lu R, Bai G, Zhang J, Deng R, et al. Genetic Variants in PCSK1 Gene Are
689 Associated with the Risk of Coronary Artery Disease in Type 2 Diabetes in a Chinese Han Population:
690 A Case Control Study. *PLOS ONE*. 2014;9(1):e87168.
- 691 31. Gjesing AP, Vestmar MA, Jørgensen T, Henri M, Holst JJ, Witte DR, et al. The Effect of PCSK1
692 Variants on Waist, Waist-Hip Ratio and Glucose Metabolism Is Modified by Sex and Glucose
693 Tolerance Status. *PLOS ONE*. 2011;6(9):e23907.
- 694 32. Nead KT, Li A, Wehner MR, Neupane B, Gustafsson S, Butterworth A, et al. Contribution of
695 common non-synonymous variants in PCSK1 to body mass index variation and risk of obesity: a
696 systematic review and meta-analysis with evidence from up to 331 175 individuals. (1460-2083
697 (Electronic)).
- 698 33. Ryan DH. Next Generation Antiobesity Medications: Setmelanotide, Semaglutide, Tirzepatide
699 and Bimagramab: What do They Mean for Clinical Practice? *J Obes Metab Syndr*. 2021;30(3):196-
700 208.
- 701 34. Blois SM, Dveksler G, Vasta GR, Freitag N, Blanchard V, Barrientos G. Pregnancy
702 Galectinology: Insights Into a Complex Network of Glycan Binding Proteins. (1664-3224 (Electronic)).
- 703 35. Schrader S, Unverdorben L, Hutter S, Knabl J, Schmoeckel E, Meister S, et al. Overexpression
704 of galectin-4 in placentas of women with gestational diabetes. (1872-7603 (Electronic)).
- 705 36. Ajayi F, Kongoasa N, Gaffey T, Asmann YW, Watson WJ, Baldi A, et al. Elevated expression of
706 serine protease HtrA1 in preeclampsia and its role in trophoblast cell migration and invasion. *Am J*
707 *Obstet Gynecol*. 2008;199(5):557.e1-10.
- 708 37. Vukojević K, Šoljić V, Martinović V, Raguž F, Filipović N. The Ubiquitin-Associated and SH3
709 Domain-Containing Proteins (UBASH3) Family in Mammalian Development and Immune Response.
710 *Int J Mol Sci*. 2024;25(3).
- 711 38. Pena LD, van Calcar SC, Hansen J, Edick MJ, Walsh Vockley C, Leslie N, et al. Outcomes and
712 genotype-phenotype correlations in 52 individuals with VLCAD deficiency diagnosed by NBS and
713 enrolled in the IBEM-IS database. *Mol Genet Metab*. 2016;118(4):272-81.
- 714 39. Hoggard N, Hunter L, Duncan JS, Williams LM, Trayhurn P, Mercer JG. Leptin and leptin
715 receptor mRNA and protein expression in the murine fetus and placenta. *Proceedings of*
716 *the National Academy of Sciences*. 1997;94(20):11073-8.
- 717 40. Kilpeläinen TO, Carli JFM, Skowronski AA, Sun Q, Kriebel J, Feitosa MF, et al. Genome-wide
718 meta-analysis uncovers novel loci influencing circulating leptin levels. *Nature Communications*.
719 2016;7(1):10494.
- 720 41. Agrawal S, Cerdeira AS, Redman C, Vatish M. Meta-Analysis and Systematic Review to Assess
721 the Role of Soluble FMS-Like Tyrosine Kinase-1 and Placenta Growth Factor Ratio in Prediction of
722 Preeclampsia: The SaPPPhirE Study. (1524-4563 (Electronic)).
- 723 42. Andrikos AA-OX, Andrikos D, Schmidt B, Birdir C, Kimmig R, Gellhaus A, et al. Course of the
724 sFlt-1/PlGF ratio in fetal growth restriction and correlation with biometric measurements, fetu-
725 maternal Doppler parameters and time to delivery. (1432-0711 (Electronic)).
- 726 43. Chang Y-S, Chen C-N, Jeng S-F, Su Y-N, Chen C-Y, Chou H-C, et al. The sFlt-1/PlGF ratio as a
727 predictor for poor pregnancy and neonatal outcomes. *Pediatrics & Neonatology*. 2017;58(6):529-33.
- 728 44. Suhre K, McCarthy MI, Schwenk JM. Genetics meets proteomics: perspectives for large
729 population-based studies. *Nature Reviews Genetics*. 2021;22(1):19-37.

730 45. Fauman EB, Hyde C. An optimal variant to gene distance window derived from an empirical
731 definition of cis and trans protein QTLs. BMC Bioinformatics. 2022;23(1):169.
732 46. Zhao J, Stewart ID, Baird D, Mason D, Wright J, Zheng J, et al. Causal effects of maternal
733 circulating amino acids on offspring birthweight: a Mendelian randomisation study. (2352-3964
734 (Electronic)).

735 Supplementary

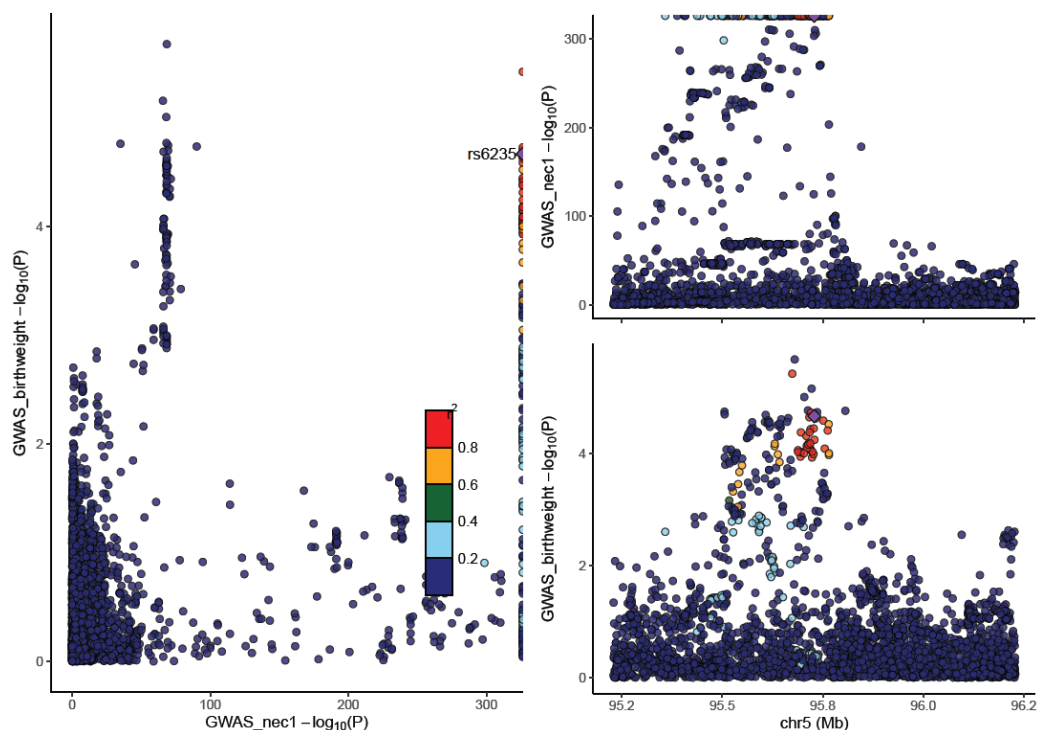
736



737

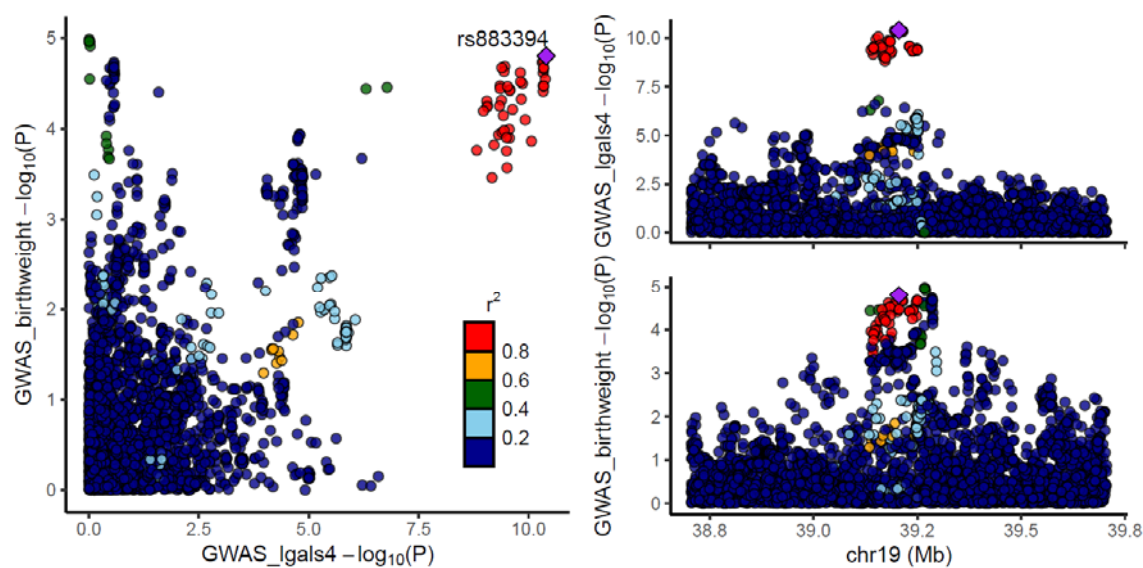
738

739 Supplementary figure 1 – a workflow of instruments (pQTL) used in our analysis.
740 Abbreviations: pQTL, protein quantitative trait loci



741

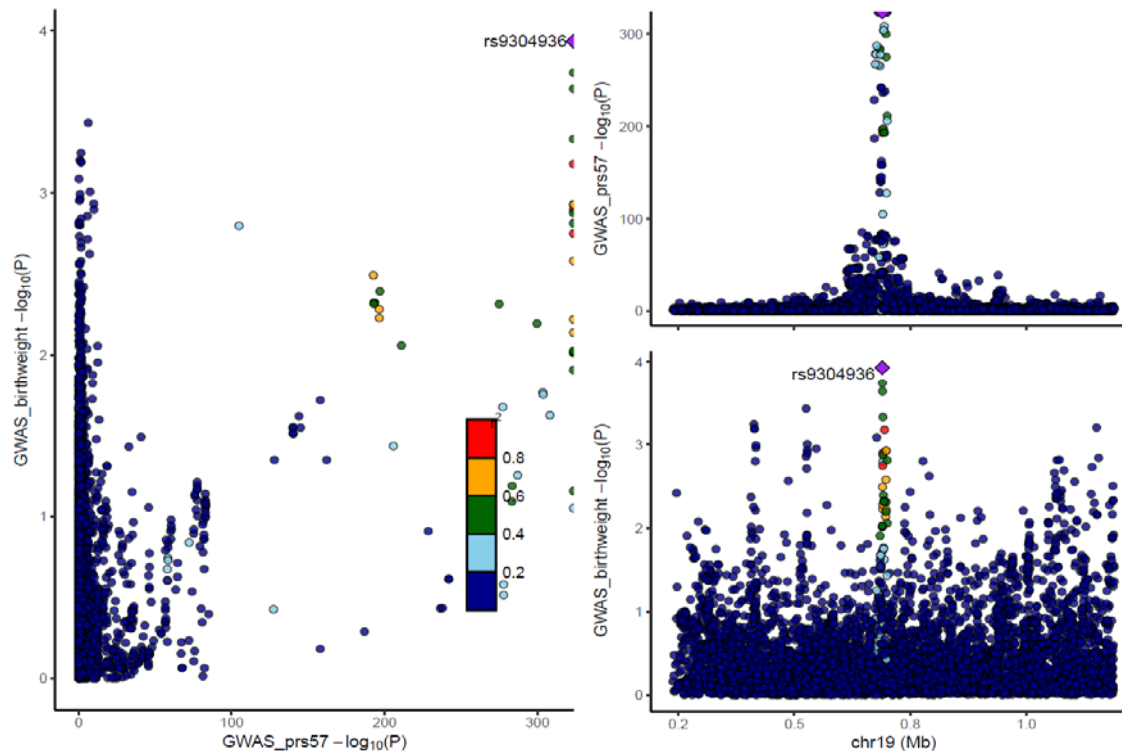
742 Supplementary figure 2 - Genetic associations with NEC1 and offspring birth weight
743 in maternal analysis. Each data point represents one genetic variant. The purple
744 diamond represents the selected pQTL. Colours indicate the R^2 values for strength
745 of linkage disequilibrium between the genetic variant and the pQTL. In the left panel,
746 the plot shows the correlation between log 10 p-values for the genetic association
747 with protein levels (x axis) and birth weight (y axis). The right panels show
748 recombination plots for the protein (top panel) and birth weight (bottom panel) with
749 log10 p-values in the y axis and chromosome positions in the x axis.



750

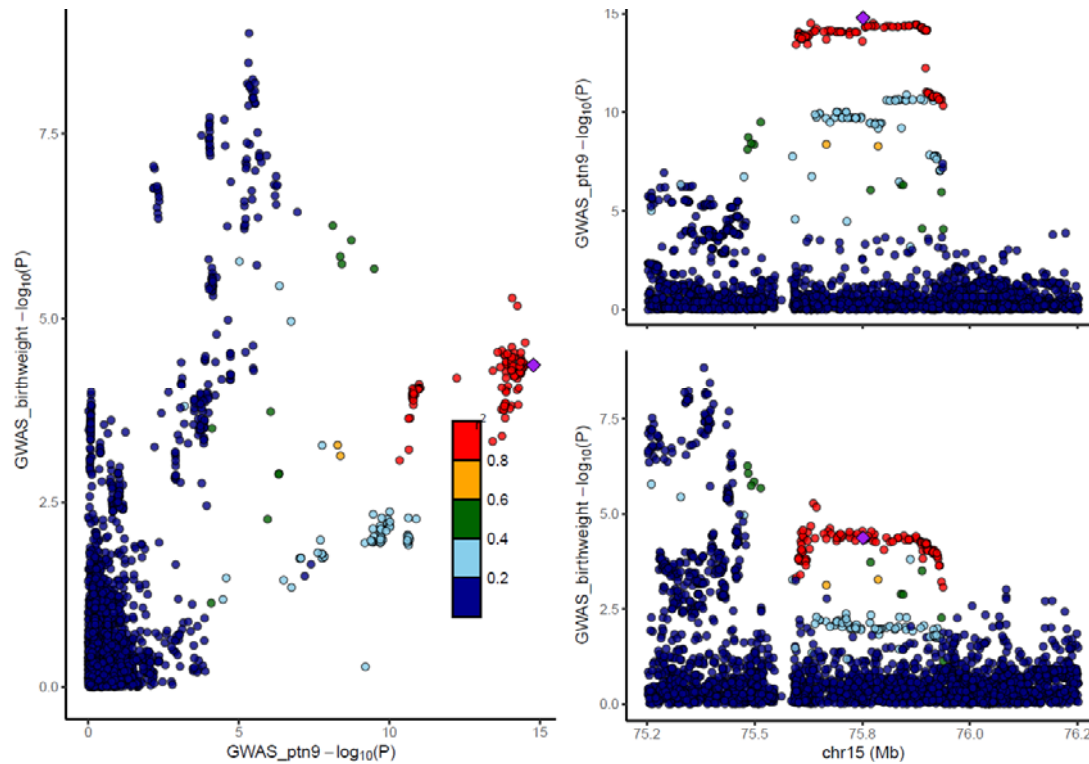
751 Supplementary figure 3 - Genetic associations with Galectin_4 and offspring birth
752 weight in maternal analysis. Each data point represents one genetic variant. The
753 purple diamond represents the selected pQTL. Colours indicate the R^2 values for

754 strength of linkage disequilibrium between the genetic variant and the pQTL. In the
755 left panel, the plot shows the correlation between log 10 p-values for the genetic
756 association with protein levels (x axis) and birth weight (y axis). The right panels
757 show recombination plots for the protein (top panel) and birth weight (bottom panel)
758 with log10 p-values in the y axis and chromosome positions in the x axis.



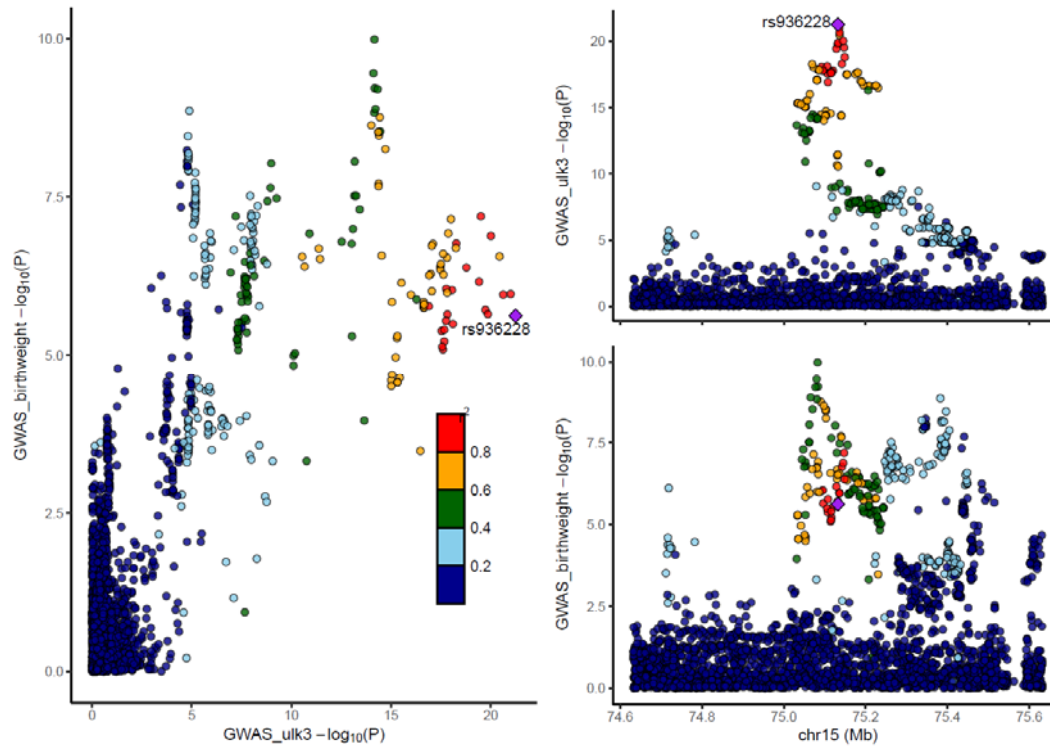
759

760 Supplementary figure 4 - Genetic associations with PRS57 and offspring birth weight
761 in maternal analysis. Each data point represents one genetic variant. The purple
762 diamond represents the selected pQTL. Colours indicate the R^2 values for strength
763 of linkage disequilibrium between the genetic variant and the pQTL. In the left panel,
764 the plot shows the correlation between log 10 p-values for the genetic association
765 with protein levels (x axis) and birth weight (y axis). The right panels show
766 recombination plots for the protein (top panel) and birth weight (bottom panel) with
767 log10 p-values in the y axis and chromosome positions in the x axis.



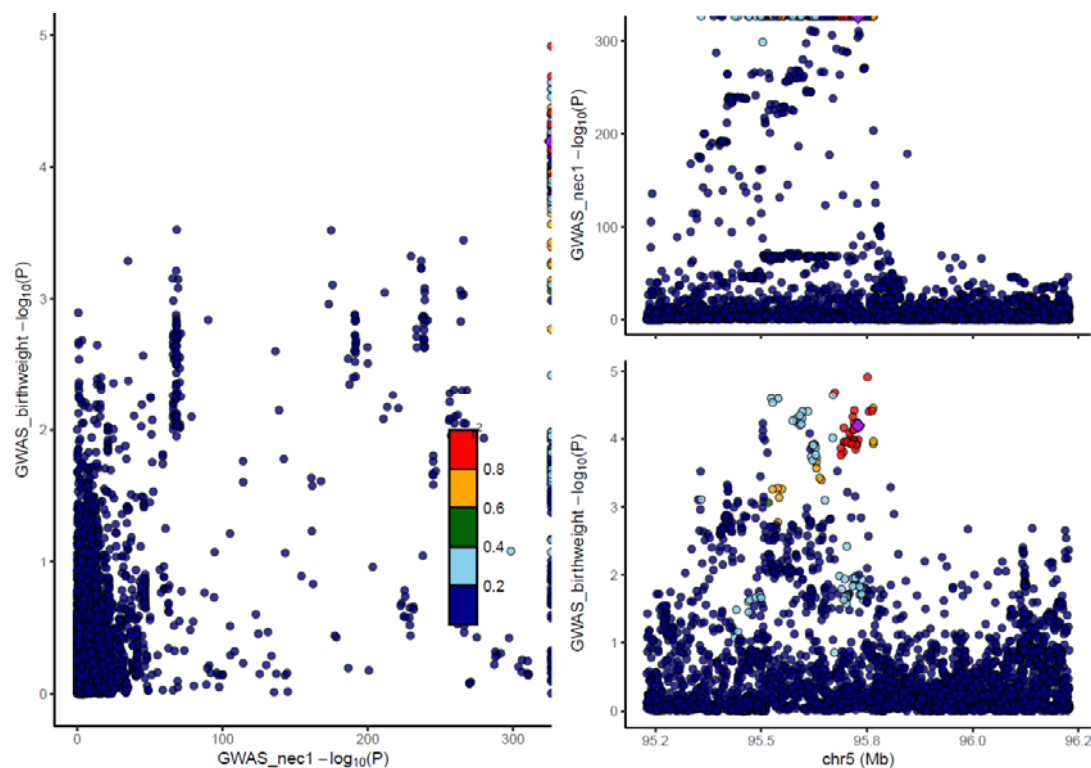
768

769 Supplementary figure 5 - Genetic associations with PTN9 and offspring birth weight
770 in offspring analyses. Each data point represents one genetic variant. The purple
771 diamond represents the selected pQTL. Colours indicate the R^2 values for strength
772 of linkage disequilibrium between the genetic variant and the pQTL. In the left panel,
773 the plot shows the correlation between log 10 p-values for the genetic association
774 with protein levels (x axis) and birth weight (y axis). The right panels show
775 recombination plots for the protein (top panel) and birth weight (bottom panel) with
776 log10 p-values in the y axis and chromosome positions in the x axis.



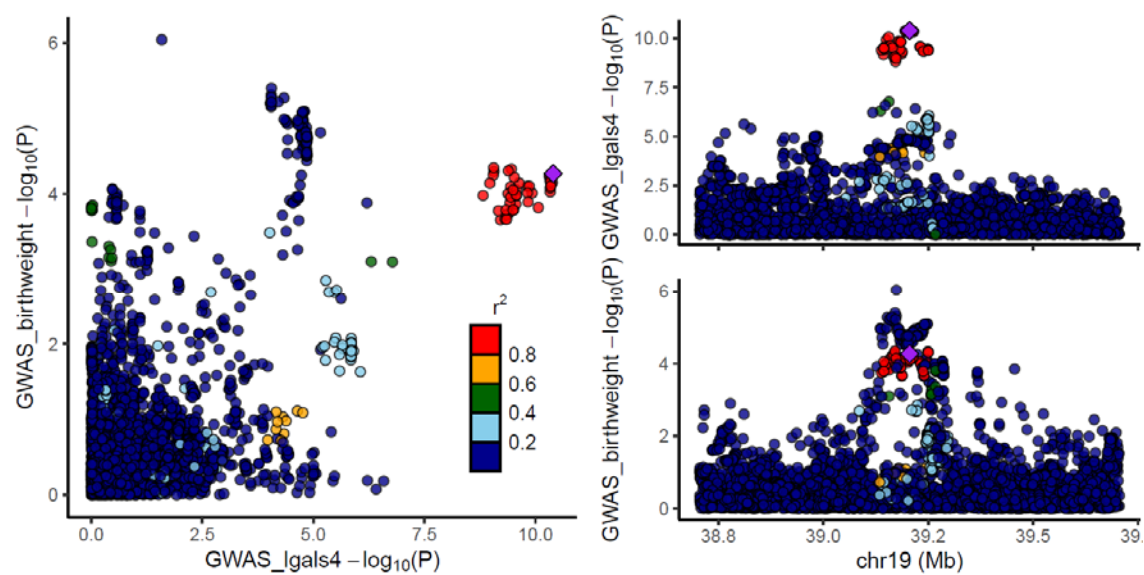
777

778 Supplementary figure 6 - Genetic associations with ULK3 and offspring birth weight
779 in maternal analysis. Each data point represents one genetic variant. The purple
780 diamond represents the selected pQTL. Colours indicate the R^2 values for strength
781 of linkage disequilibrium between the genetic variant and the pQTL. In the left panel,
782 the plot shows the correlation between \log_{10} p-values for the genetic association
783 with protein levels (x axis) and birth weight (y axis). The right panels show
784 recombination plots for the protein (top panel) and birth weight (bottom panel) with
785 \log_{10} p-values in the y axis and chromosome positions in the x axis.



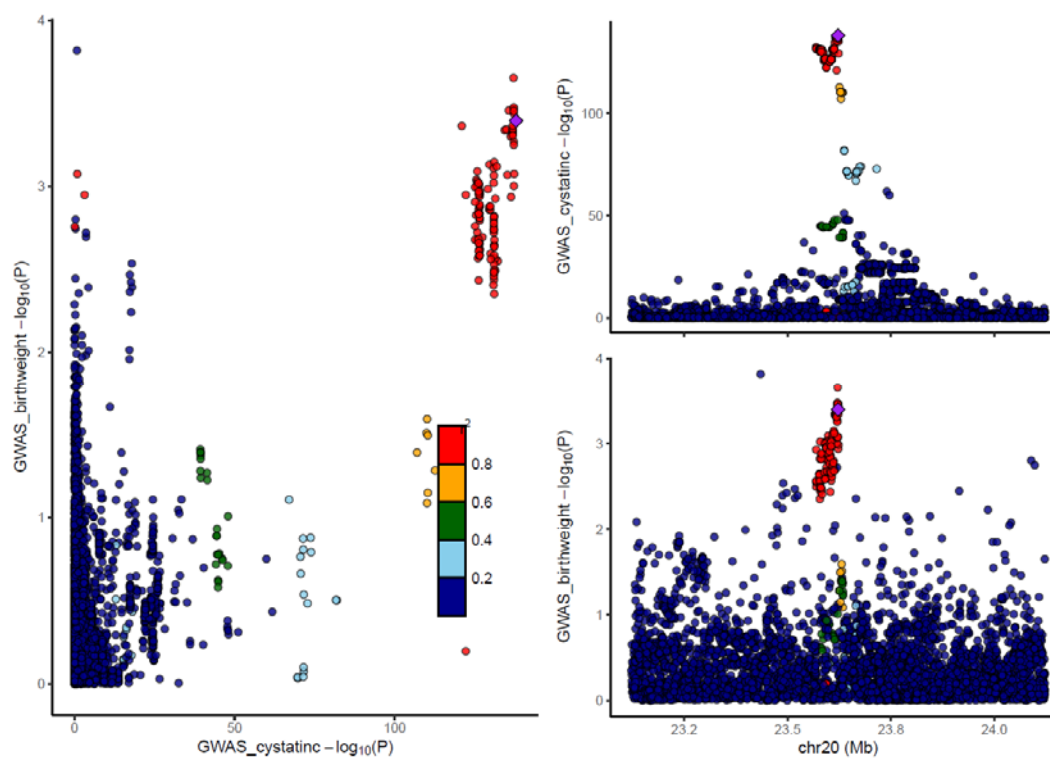
786

787 Supplementary figure 7 - Genetic associations with NEC1 and offspring birth weight
788 in offspring analysis. Each data point represents one genetic variant. The purple
789 diamond represents the selected pQTL. Colours indicate the R^2 values for strength
790 of linkage disequilibrium between the genetic variant and the pQTL. In the left panel,
791 the plot shows the correlation between log 10 p-values for the genetic association
792 with protein levels (x axis) and birth weight (y axis). The right panels show
793 recombination plots for the protein (top panel) and birth weight (bottom panel) with
794 log10 p-values in the y axis and chromosome positions in the x axis.



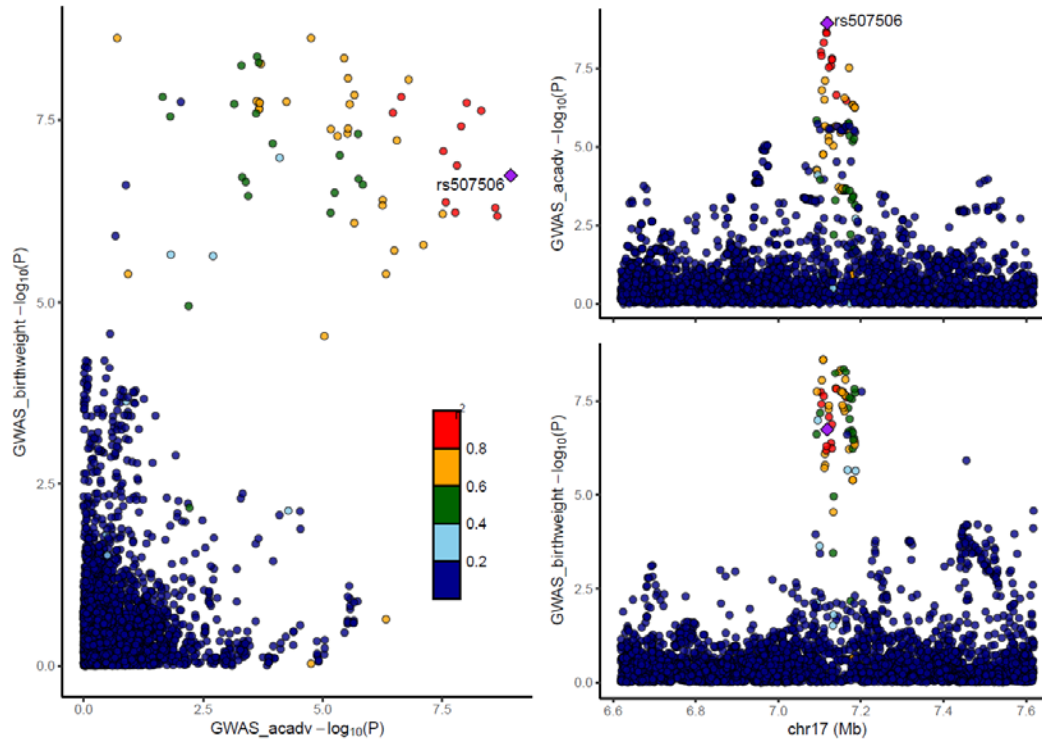
795

796 Supplementary figure 8 - Genetic associations with Galectin_4 and offspring birth
797 weight in offspring analysis. Each data point represents one genetic variant. The
798 purple diamond represents the selected pQTL. Colours indicate the R^2 values for
799 strength of linkage disequilibrium between the genetic variant and the pQTL. In the
800 left panel, the plot shows the correlation between log 10 p-values for the genetic
801 association with protein levels (x axis) and birth weight (y axis). The right panels
802 show recombination plots for the protein (top panel) and birth weight (bottom panel)
803 with log10 p-values in the y axis and chromosome positions in the x axis.



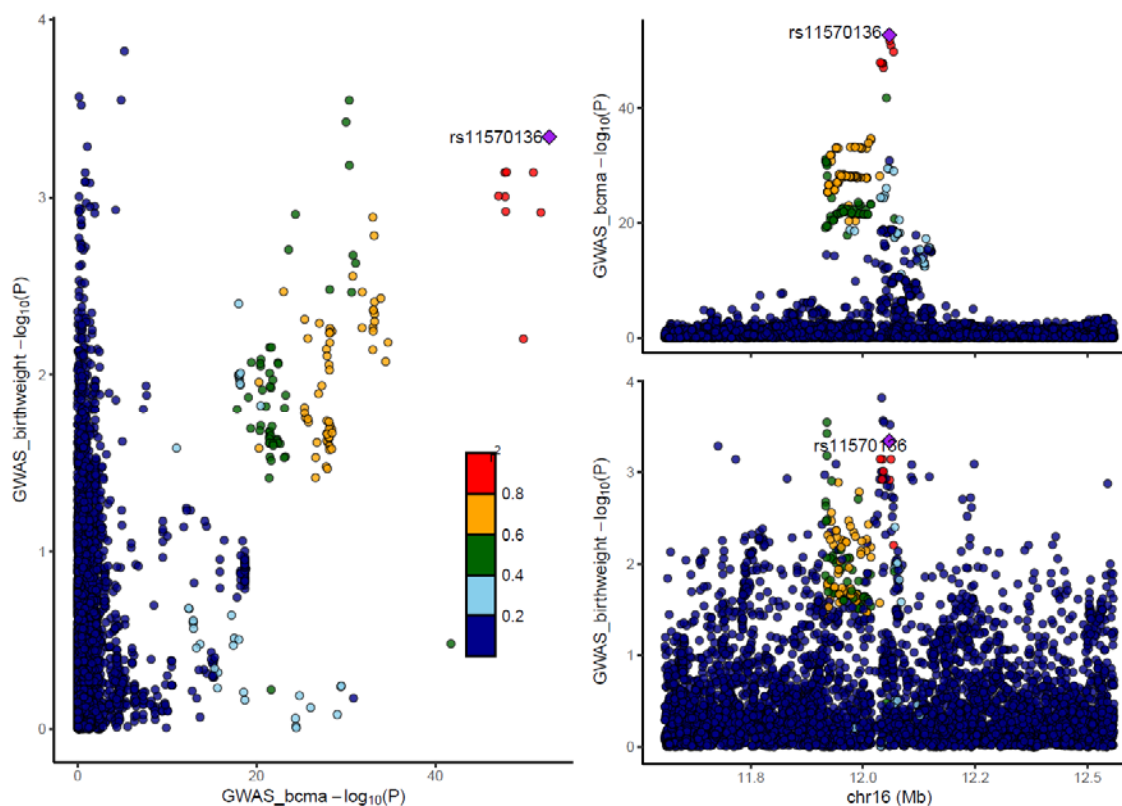
804

805 Supplementary figure 9 - Genetic associations with Cystatin_c and offspring birth
806 weight in offspring analysis. Each data point represents one genetic variant. The
807 purple diamond represents the selected pQTL. Colours indicate the R^2 values for
808 strength of linkage disequilibrium between the genetic variant and the pQTL. In the
809 left panel, the plot shows the correlation between log 10 p-values for the genetic
810 association with protein levels (x axis) and birth weight (y axis). The right panels
811 show recombination plots for the protein (top panel) and birth weight (bottom panel)
812 with log10 p-values in the y axis and chromosome positions in the x axis.



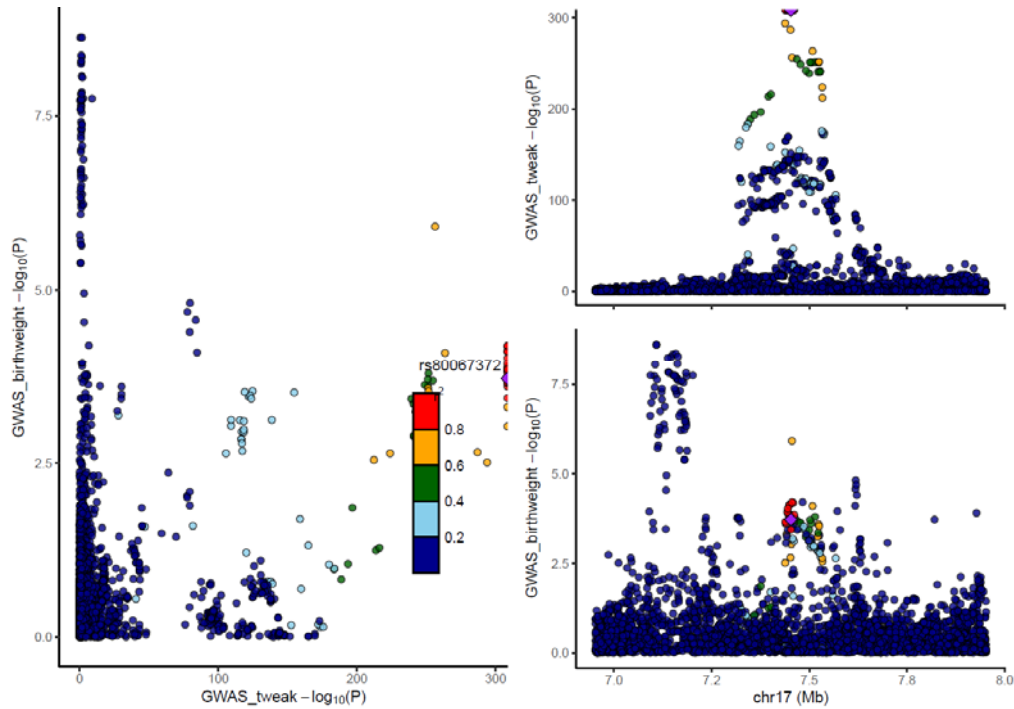
813

814 Supplementary figure 10 - Genetic associations with ACADV and offspring birth
815 weight in offspring analysis. Each data point represents one genetic variant. The
816 purple diamond represents the selected pQTL. Colours indicate the R^2 values for
817 strength of linkage disequilibrium between the genetic variant and the pQTL. In the
818 left panel, the plot shows the correlation between log 10 p-values for the genetic
819 association with protein levels (x axis) and birth weight (y axis). The right panels
820 show recombination plots for the protein (top panel) and birth weight (bottom panel)
821 with log10 p-values in the y axis and chromosome positions in the x axis.



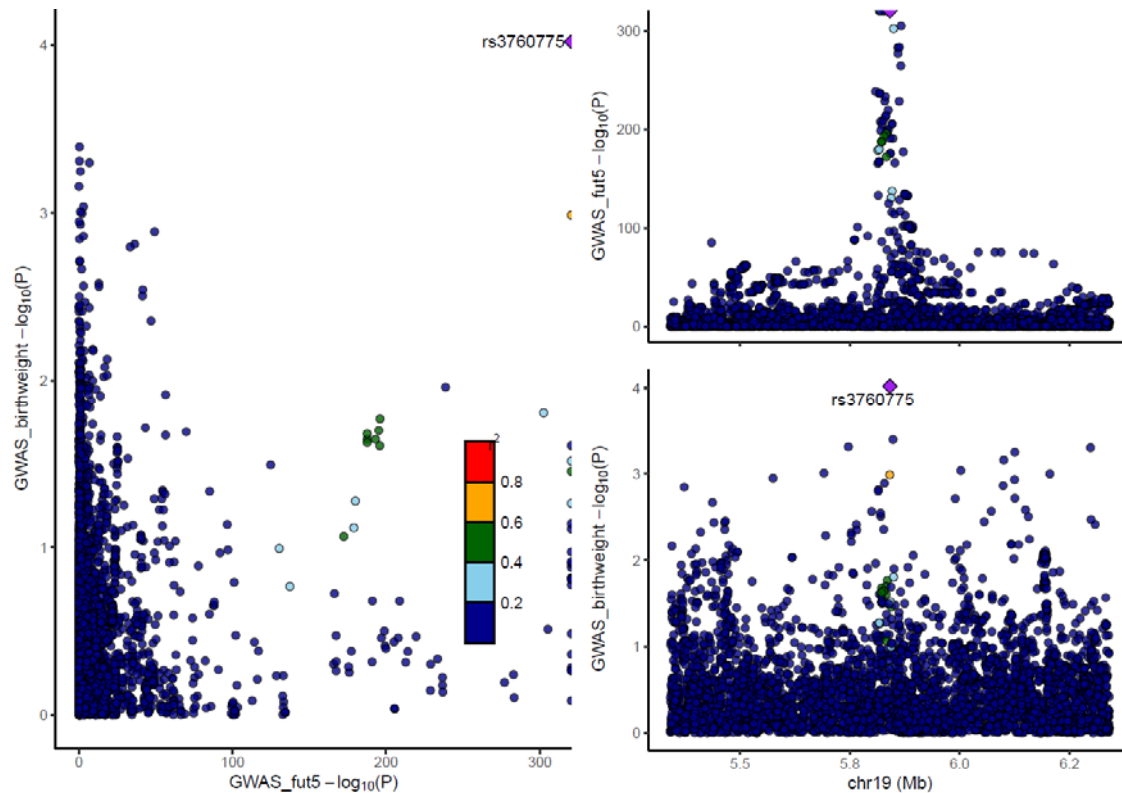
822

823 Supplementary figure 11 - Genetic associations with BCMA and offspring birth
824 weight in offspring analysis. Each data point represents one genetic variant. The
825 purple diamond represents the selected pQTL. Colours indicate the R^2 values for
826 strength of linkage disequilibrium between the genetic variant and the pQTL. In the
827 left panel, the plot shows the correlation between \log_{10} p-values for the genetic
828 association with protein levels (x axis) and birth weight (y axis). The right panels
829 show recombination plots for the protein (top panel) and birth weight (bottom
830 panel) with \log_{10} p-values in the y axis and chromosome positions in the x axis.



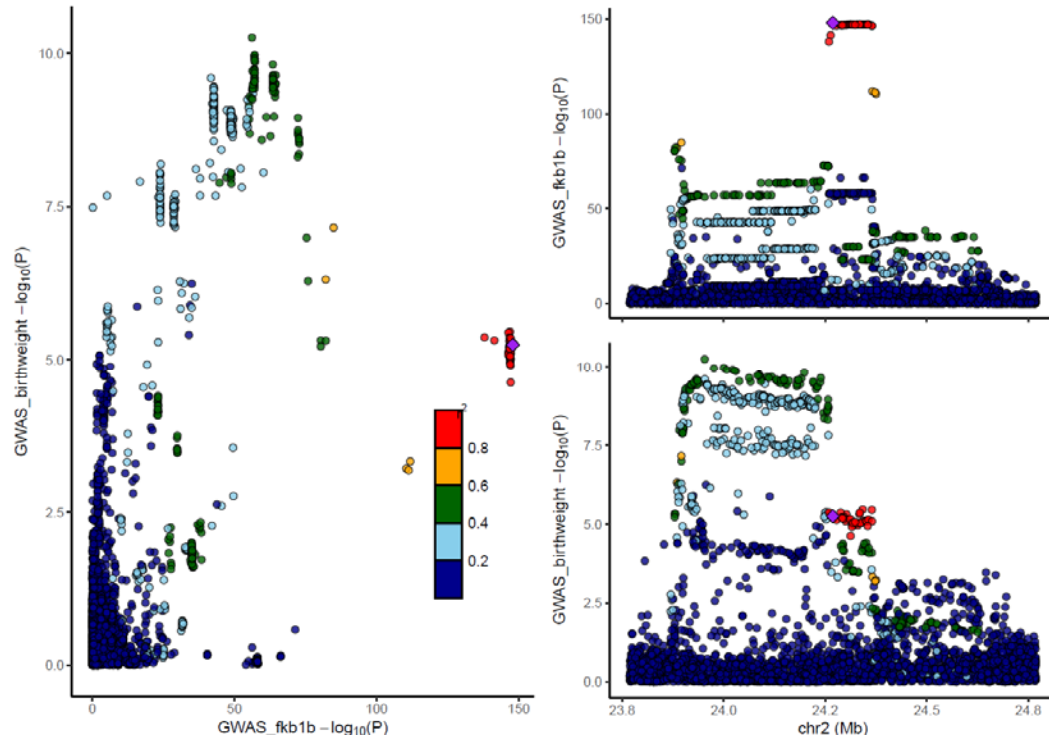
831

832 Supplementary figure 12 - Genetic associations with TWEAK and offspring birth
833 weight in offspring analysis. Each data point represents one genetic variant. The
834 purple diamond represents the selected pQTL. Colours indicate the R² values for
835 strength of linkage disequilibrium between the genetic variant and the pQTL. In the
836 left panel, the plot shows the correlation between log 10 p-values for the genetic
837 association with protein levels (x axis) and birth weight (y axis). The right panels
838 show recombination plots for the protein (top panel) and birth weight (bottom panel)
839 with log10 p-values in the y axis and chromosome positions in the x axis.



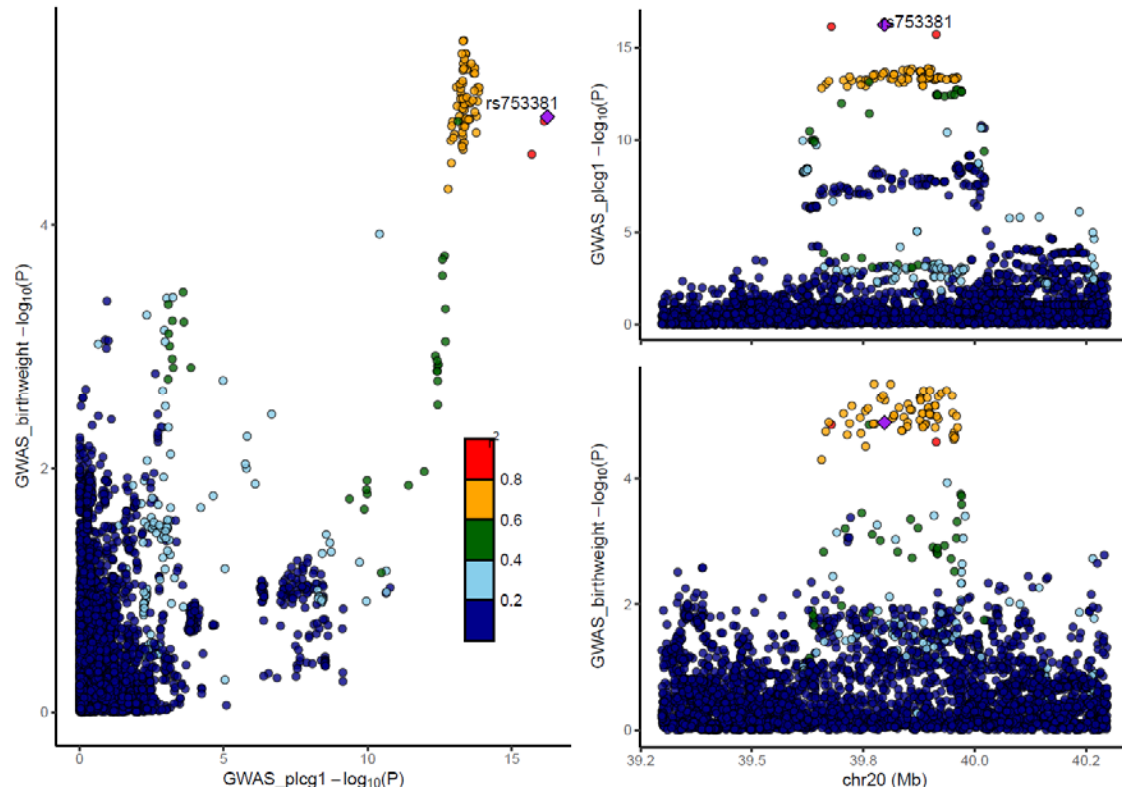
840

841 Supplementary figure 13 - Genetic associations with FUT5 and offspring birth weight
842 in offspring analysis. Each data point represents one genetic variant. The purple
843 diamond represents the selected pQTL. Colours indicate the R^2 values for strength
844 of linkage disequilibrium between the genetic variant and the pQTL. In the left panel,
845 the plot shows the correlation between \log_{10} p-values for the genetic association
846 with protein levels (x axis) and birth weight (y axis). The right panels show
847 recombination plots for the protein (top panel) and birth weight (bottom panel) with
848 \log_{10} p-values in the y axis and chromosome positions in the x axis.



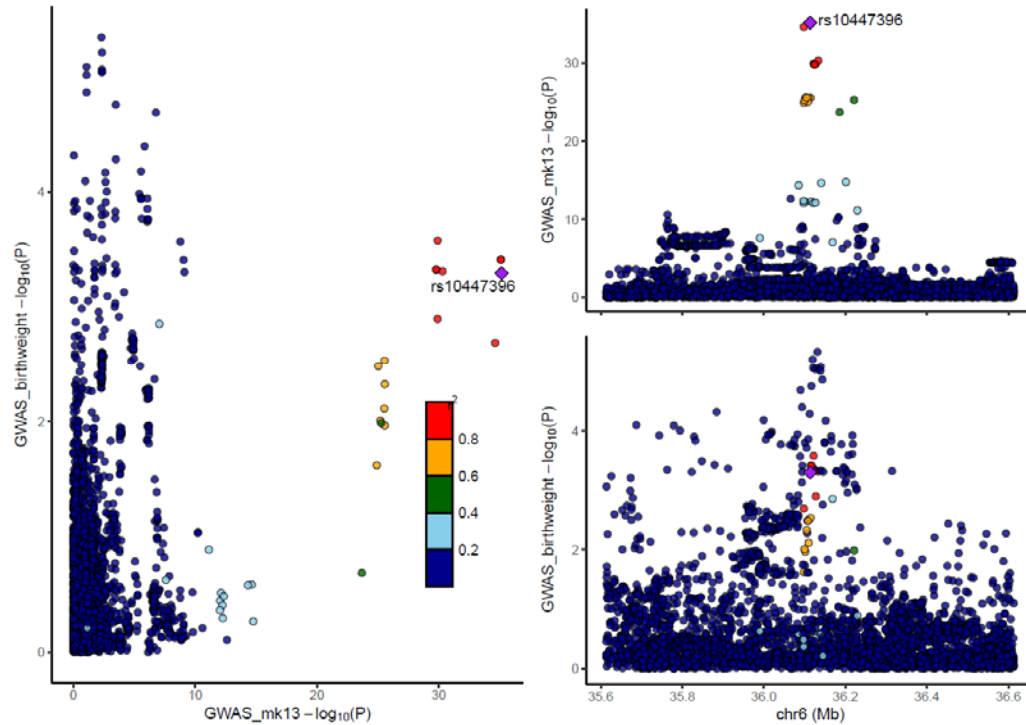
849

850 Supplementary figure 14 - Genetic associations with FKB1B and offspring birth
851 weight in offspring analysis. Each data point represents one genetic variant. The
852 purple diamond represents the selected pQTL. Colours indicate the R² values for
853 strength of linkage disequilibrium between the genetic variant and the pQTL. In the
854 left panel, the plot shows the correlation between log 10 p-values for the genetic
855 association with protein levels (x axis) and birth weight (y axis). The right panels
856 show recombination plots for the protein (top panel) and birth weight (bottom panel)
857 with log10 p-values in the y axis and chromosome positions in the x axis.



858

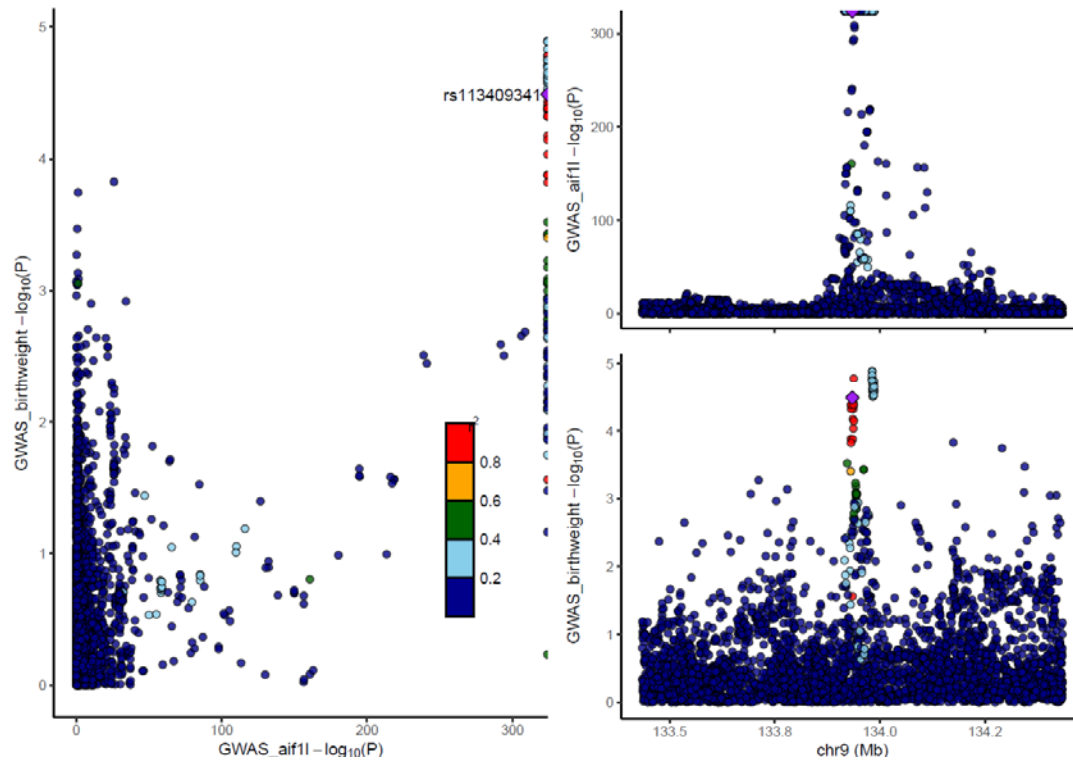
859 Supplementary figure 15 - Genetic associations with PLCG1 and offspring birth
860 weight in offspring analysis. Each data point represents one genetic variant. The
861 purple diamond represents the selected pQTL. Colours indicate the R² values for
862 strength of linkage disequilibrium between the genetic variant and the pQTL. In the
863 left panel, the plot shows the correlation between log 10 p-values for the genetic
864 association with protein levels (x axis) and birth weight (y axis). The right panels
865 show recombination plots for the protein (top panel) and birth weight (bottom panel)
866 with log10 p-values in the y axis and chromosome positions in the x axis.



867

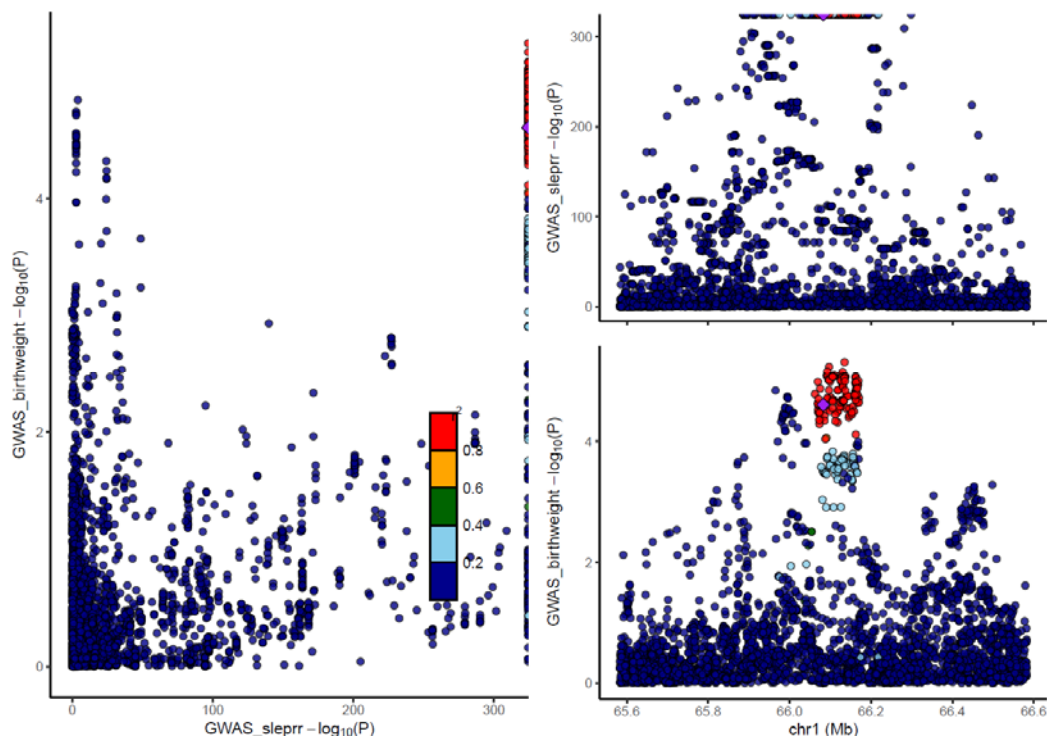
868 Supplementary figure 16 - Genetic associations with MK13 and offspring birth weight
869 in offspring analysis. Each data point represents one genetic variant. The purple
870 diamond represents the selected pQTL. Colours indicate the R^2 values for strength
871 of linkage disequilibrium between the genetic variant and the pQTL. In the left panel,
872 the plot shows the correlation between \log_{10} p-values for the genetic association
873 with protein levels (x axis) and birth weight (y axis). The right panels show
874 recombination plots for the protein (top panel) and birth weight (bottom panel) with
875 \log_{10} p-values in the y axis and chromosome positions in the x axis.

876



877

878 Supplementary figure 18 - Genetic associations with AIF1L and offspring birth weight
879 in offspring analysis. Each data point represents one genetic variant. The purple
880 diamond represents the selected pQTL. Colours indicate the R^2 values for strength
881 of linkage disequilibrium between the genetic variant and the pQTL. In the left panel,
882 the plot shows the correlation between \log_{10} p-values for the genetic association
883 with protein levels (x axis) and birth weight (y axis). The right panels show
884 recombination plots for the protein (top panel) and birth weight (bottom panel) with
885 \log_{10} p-values in the y axis and chromosome positions in the x axis.



886

887 Supplementary figure 19 - Genetic associations with sLeptin_R and offspring birth
888 weight in offspring analysis. Each data point represents one genetic variant. The
889 purple diamond represents the selected pQTL. Colours indicate the R² values for
890 strength of linkage disequilibrium between the genetic variant and the pQTL. In the
891 left panel, the plot shows the correlation between log 10 p-values for the genetic
892 association with protein levels (x axis) and birth weight (y axis). The right panels
893 show recombination plots for the protein (top panel) and birth weight (bottom panel)
894 with log10 p-values in the y axis and chromosome positions in the x axis.

895

896

897

898

899

900

901

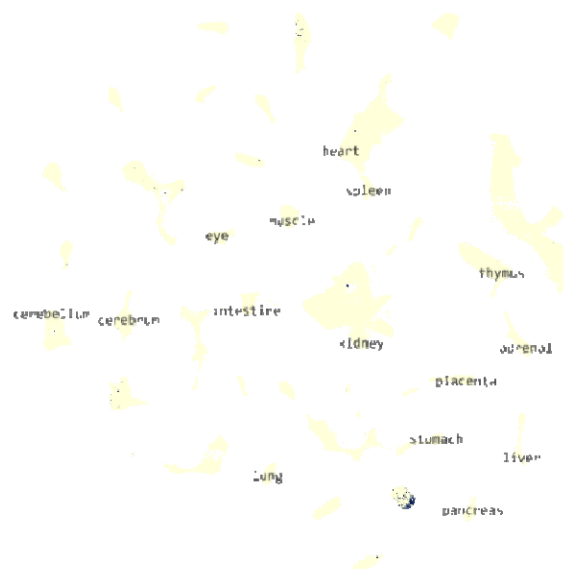
902

903

904

905

906



907

908 Supplementary figure 20 - Fetal single cell gene expression expressed in the
909 pancreas for NEC1, where the organs are shown in yellow and the single cells
910 demonstrating expression in navy blue.



911

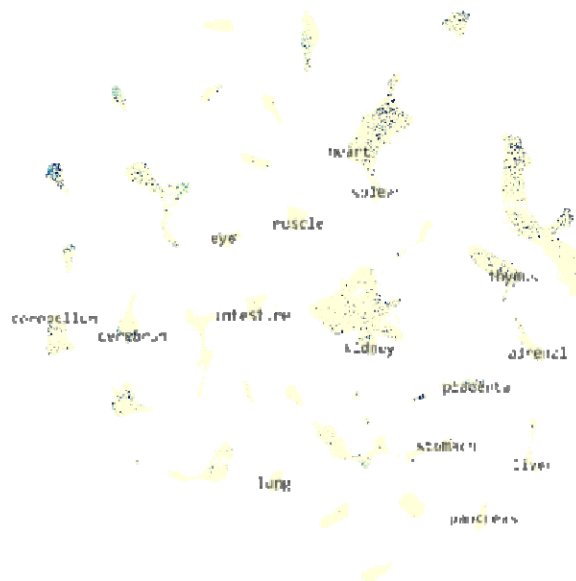
912 Supplementary figure 22 - Fetal single cell gene expression expressed tissue-wide
913 for Galectin_4, where the organs are shown in yellow and the single cells
914 demonstrating expression in navy blue.

915



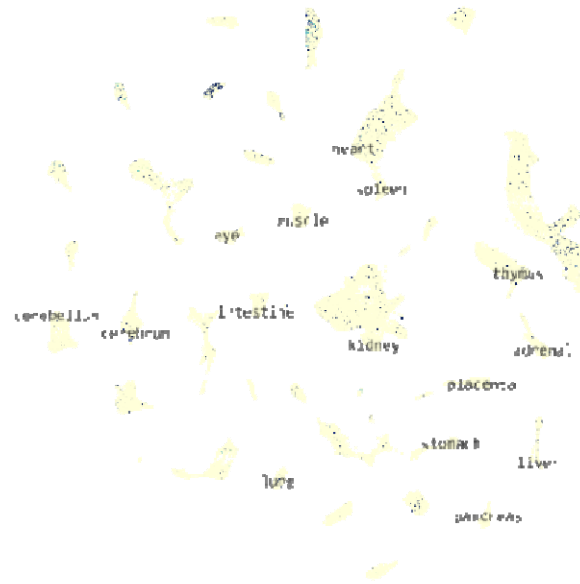
916

917 Supplementary figure 23 - Fetal single cell gene expression expressed tissue-wide
918 for FUT5, where the organs are shown in yellow and the single cells demonstrating
919 expression in navy blue.



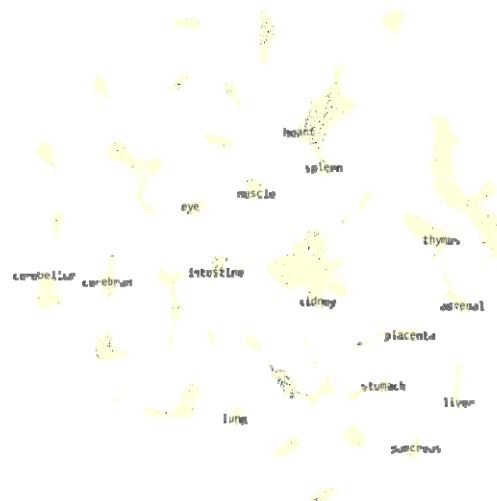
920

921 Supplementary figure 24 - Fetal single cell gene expression expressed tissue-wide
922 for UBS3B, where the organs are shown in yellow and the single cells demonstrating
923 expression in navy blue.



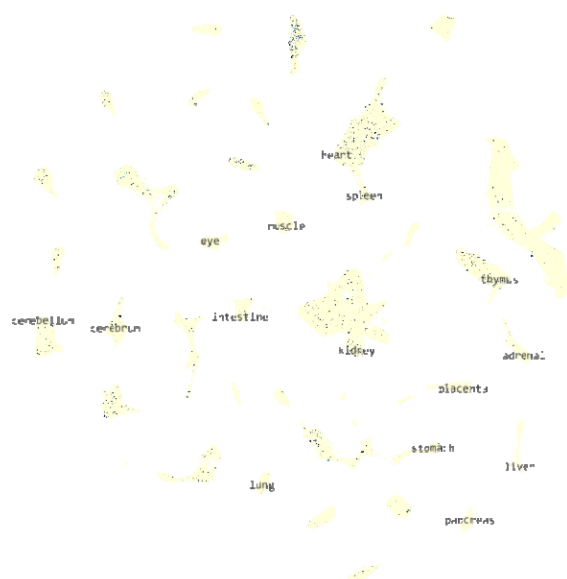
924

925 Supplementary figure 25 - Fetal single cell gene expression expressed tissue-wide
926 for sLeptin_R, where the organs are shown in yellow and the single cells
927 demonstrating expression in navy blue.



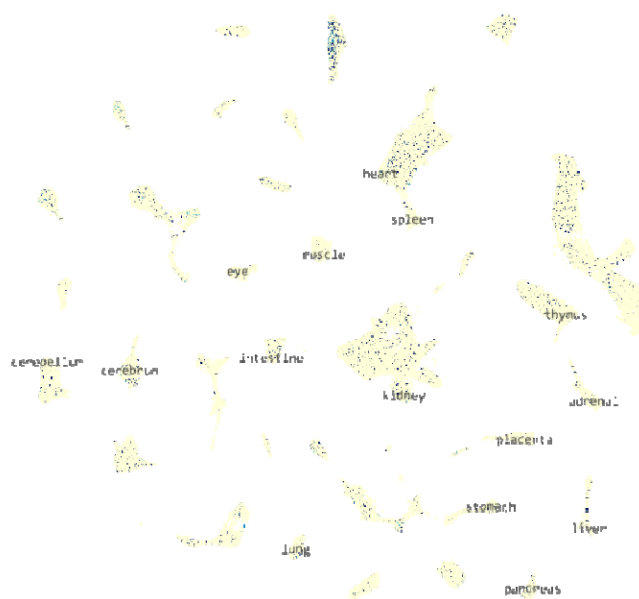
928

929 Supplementary figure 26 - Fetal single cell gene expression expressed tissue-wide
930 for AIF1L, where the organs are shown in yellow and the single cells demonstrating
931 expression in navy blue.



932

933 Supplementary figure 27 - Fetal single cell gene expression expressed tissue-wide
934 for PLCG1, where the organs are shown in yellow and the single cells demonstrating
935 expression in navy blue.



936

937 Supplementary figure 28 - Fetal single cell gene expression expressed tissue-wide
938 for IFN_a_b_R1, where the organs are shown in yellow and the single cells
939 demonstrating expression in navy blue.



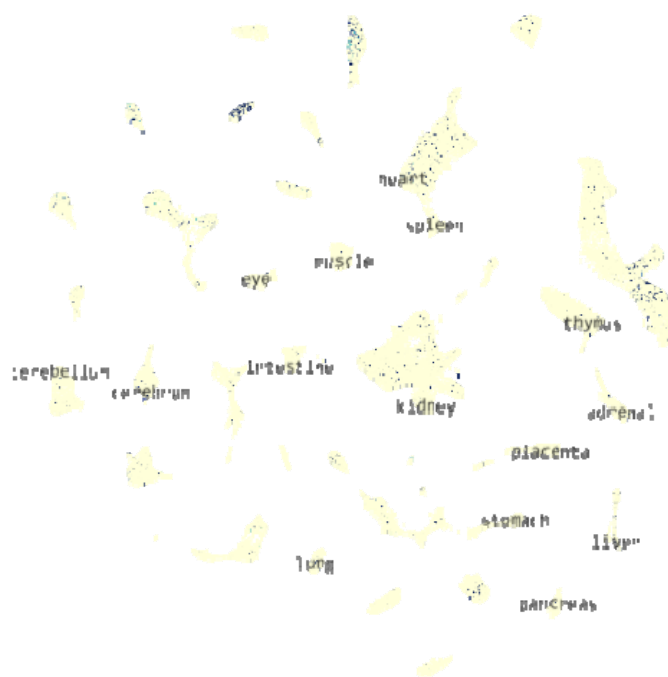
940

941 Supplementary figure 29 - Fetal single cell gene expression expressed tissue-wide
942 for ACADV, where the organs are shown in yellow and the single cells demonstrating
943 expression in navy blue.

944

945

946



947

948 Supplementary figure 22 - Fetal single cell gene expression expressed tissue-wide
949 for sLeptin_R, where the organs are shown in yellow and the single cells
950 demonstrating expression in navy blue.

951

952

953

954

955

956

957

958

959